AD-A078 816 VARIAN ASSOCIATES INC PALO ALTO CA F/G 20/12
RESEARCH ON INGAAS FET'S.(U)
UNCLASSIFIED SEP 79 S BANDY , T BOYLE , R FULKS , S HYDER N00014-78-C-0380
TR-1 NL

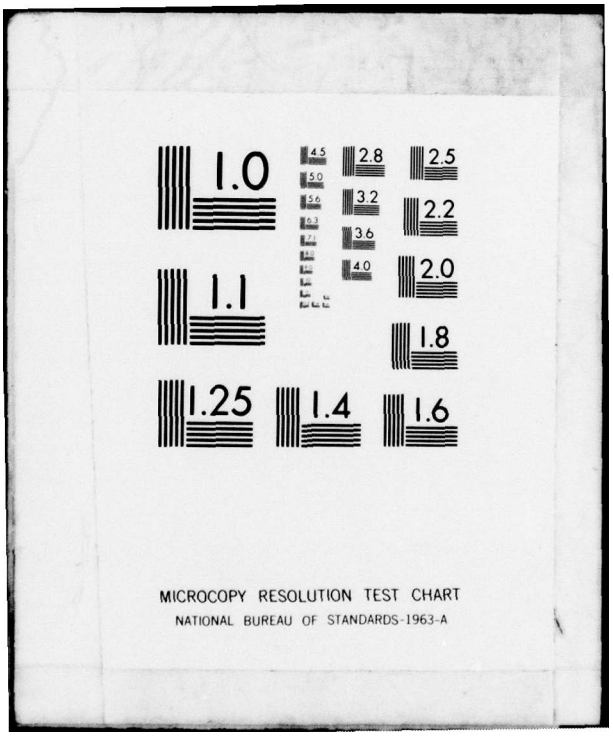
1.0
1.1
1.25
1.4
1.6
1.8
2.0
2.2
2.5
2.8
3.2
3.6
4.0
4.5
5.0
5.6
6.3
MICROCOPY RESOLUTION TEST CHART
NATIONAL BUREAU OF STANDARDS-1963-A

LEVEL II

12 B.S.

INTERIM TECHNICAL REPORT NO. 1

Research on InGaAs FET's

September 1979

Prepared by:

S. Bandy, T. Boyle, R. Fulks, S. Hyder,
C. Nishimoto, and T. Yep

VARIAN ASSOCIATES, INC.
611 Hansen Way
Palo Alto, CA 94303

This research was sponsored by
the Office of Naval Research
under Contract N00014-78-C-0380,
Contract Authority: NR 251-030

DISCLAIMER NOTICE

THIS DOCUMENT IS BEST QUALITY PRACTICABLE. THE COPY FURNISHED TO DDC CONTAINED A SIGNIFICANT NUMBER OF PAGES WHICH DO NOT REPRODUCE LEGIBLY.

UNCLASSIFIED
SECURITY CLASSIFICATION OF THIS PAGE (When Data Entered)

REPORT DOCUMENTATION PAGE

READ INSTRUCTIONS BEFORE COMPLETING FORM

1. REPORT NUMBER: Interim Technical Report No.1
2. GOVT ACCESSION NO.
3. RECIPIENT'S CATALOG NUMBER

4. TITLE (and Subtitle): (6) Research on InGaAs FET's.
5. TYPE OF REPORT & PERIOD COVERED: (9) Interim Technical rept's
6. PERFORMING ORG. REPORT NUMBER

7. AUTHOR(s): (10) S. Bandy, T. Boyle, R. Fulks, S. Hyder, C. Nishimoto and T. Yep
8. CONTRACT OR GRANT NUMBER(s): (15) N00014-78-C-0380

9. PERFORMING ORGANIZATION NAME AND ADDRESS:
Varian Associates, Inc.
611 Hansen Way
Palo Alto, CA 94303
(14) TR-1
10. PROGRAM ELEMENT, PROJECT, TASK AREA & WORK UNIT NUMBERS:
PE62762N
RF-54-581-001
NR 251-030

11. CONTROLLING OFFICE NAME AND ADDRESS:
Office of Naval Research
800 N. Quincy Street
Arlington, VA 22217
(11)
12. REPORT DATE: September 1979
13. NUMBER OF PAGES: 63

14. MONITORING AGENCY NAME & ADDRESS (if different from Controlling Office):
(16) F54581
(12) 64
15. SECURITY CLASS. (of this report): UNCLAS
15a. DECLASSIFICATION/DOWNGRADING SCHEDULE

16. DISTRIBUTION STATEMENT (of this Report):
(17) RF54581001

Approved for public release; distribution unlimited.

Reproduction in whole or in part is permitted for any purpose of the US government.

17. DISTRIBUTION STATEMENT (of the abstract entered in Block 20, if different from Report)

18. SUPPLEMENTARY NOTES

19. KEY WORDS (Continue on reverse side if necessary and identify by block number)

Schottky-barrier FET
InGaAs epitaxial growth
Saturated velocity determination
lattice mismatch
laser annealing

20. ABSTRACT (Continue on reverse side if necessary and identify by block number)

It appears that dislocation-free InGaAs grown by VPE on GaAs with In percentages above 25% can only be done through the use of an H_2 bypass for the particular reactor configuration used. All growth done without the H_2 bypass had bluish haze on the surface and low values of saturated velocity.

DD FORM 1 JAN 73 1473 EDITION OF 1 NOV 65 IS OBSOLETE

364100

UNCLASSIFIED
SECURITY CLASSIFICATION OF THIS PAGE (When Data Entered)

Vapor Phase Epitaxy

SUMMARY

Field Effect Transistors

Virtually the whole effort for this period was spent in trying to grow by (VPE) dislocation-free InGaAs on GaAs at In percentages above 25%. Of all the techniques tried, significant improvement came only after installation of a H_2 bypass on the reactor. FETs fabricated on the best of the pre-H_2 bypass wafers showed sub-GaAs values for the effective saturated velocity, and FETs have yet to be fabricated on the wafers grown with the H_2 bypass. Efforts at ion-implanting the pre-H_2 bypass wafers were not successful, presumably because of the heavy amount of dislocations in the material.

1. INTRODUCTION

The contract is in essence an extension of the work begun under the ONR contract N00014-75-C-0125. The introduction of the final report of that contract[1] is repeated here for the sake of completeness, along with the salient features of that work and the intention of the work on this contract towards complementing and extending that work.

The important parameter which determines the limiting frequency response of FETs is the transit time which the electrons take to cross the active gate region. Figure 1 shows the velocity-field characteristic for $10^{17}cm^{-3}$ doped GaAs[2] and a simple two-piece fit typically used to model it. As gate lengths have progressively decreased in an effort to reduce the transit time, the electric fields in the channel exceed to a greater degree the threshold for intervalley transfer (approximately E_s in Fig. 1). Since the transit time is not large with respect to the intervalley scattering time, one must consider the actual electron dynamics rather than just the static velocity-field characteristic in estimating what FET performance will be.[3,4] This need is demonstrated by the fact that although the high field drift velocity for GaAs exceeds that for Si by only 10% at most, there is a dramatic improvement in the figure of merit f_{max}.[3]

The optimum FET material would allow the electrons to travel at the highest possible velocity in the Γ minimum (i.e. have a low Γ effective mass), and spend the longest possible time at high energies in the Γ minimum before transferring into the upper valleys (i.e. have a large

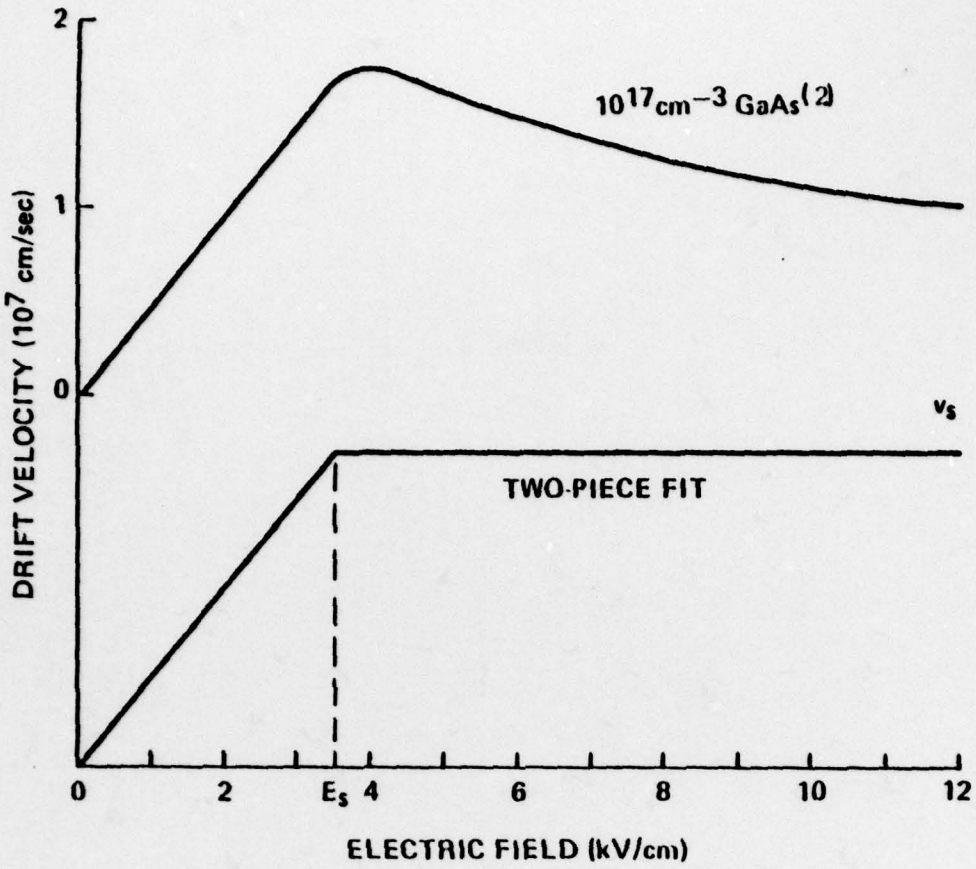

Figure 1. Velocity-field characteristic for 10^{17}cm^{-3} doped GaAs and a simple two-piece fit.

intervalley energy separation and low intervalley coupling constant). Although it appears that InP has a slightly higher peak velocity than GaAs,[5] the coupling constant for Γ to L transfer in GaAs is around 3×10^8 eV cm^{-1},[6] while that for InP is in the $5\text{-}14 \times 10^8$ range.[7] Since the scattering time goes as the inverse square of the coupling constant, the more rapid scattering of the electrons into the L valleys in InP will compensate the higher Γ to L energy separation (0.6 eV vs 0.38 eV for GaAs[6,7]) somewhat when velocity overshoot effects are taken into account.

Figure 2 shows the position of the Γ, X, and L minima for the ternary $In_xGa_{1-x}As$ as a function of x.[8-11] As In is added to GaAs the bandgap decreases, thus decreasing the Γ effective mass.[12] In addition, the Γ to L energy separation increases so that the threshold for upper valley transfer is increased, assuming that the Γ to X coupling coefficient is relatively independent of composition. This will contribute to shortening the electron transit time through the active gate region, and should lead to improved FET performance over that for GaAs. Although InGaAs has been considered previously as a candidate for an optimum material,[13] an artificial constraint of the intervalley energy separation being larger than the bandgap led to its being considered less desirable than InAsP. GaAs, the best material to date for demonstrated FET performance, does not meet this requirement, and Fig. 2 suggests that InGaAs is an improvement over GaAs with respect to this criterion.

$In_xGa_{1-x}As$ also offers the advantage of differing from GaAs only incrementally depending upon the value of x, so at least for low values of x the processing technology for GaAs

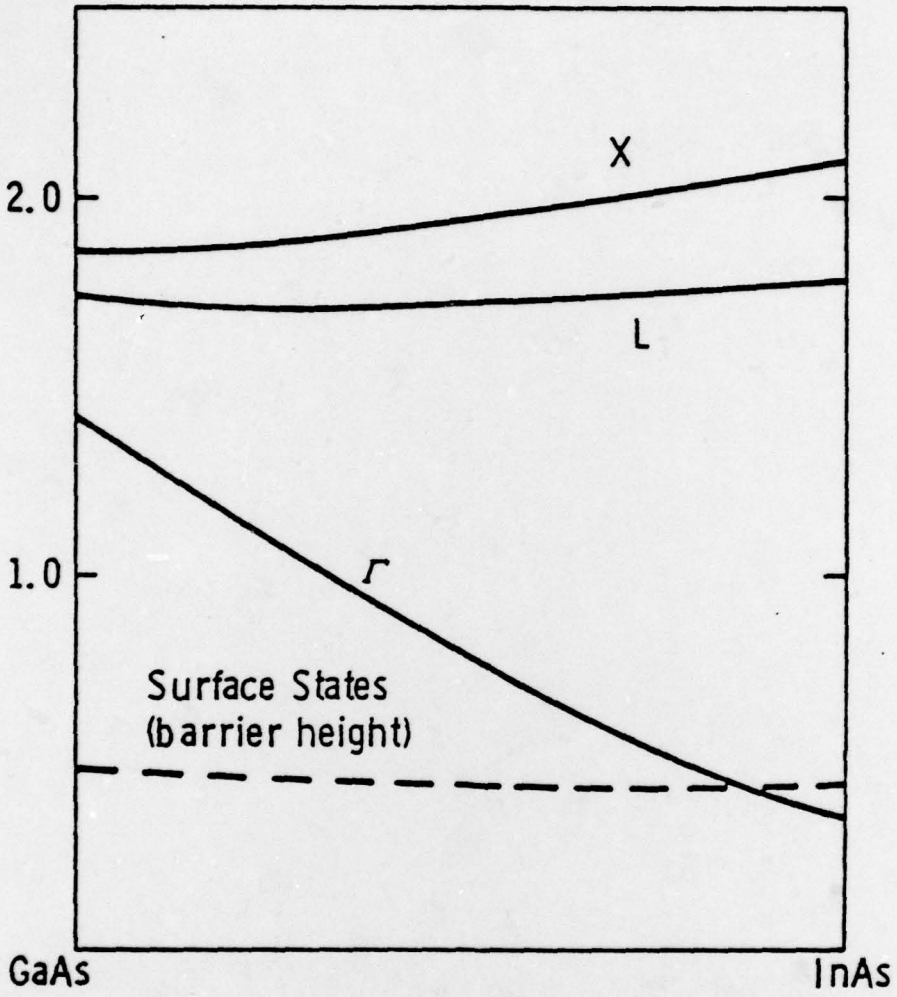

Fig. 2: Schematic of band edges for the InGaAs ternary system.

should also be suitable if not better for InGaAs (e.g. the reduced barrier height should reduce the contact resistance of the ohmic contacts). Except for the very high energy values of x, InGaAs has a barrier height advantage over InP. The technique of lattice matching InGaAs to a semi-insulating GaAs substrate by a graded region grown by VPE has been demonstrated on the previous contract,[1] enabling InGaAs to enjoy the benefits of the superior semi-insulating GaAs substrate quality over that of InP, for example.

The work on Contract N00014-75-C-0125[1] has shown an effective saturated drift velocity greater than that for GaAs for FETs fabricated using InGaAs. The most positive evidence was obtained from a device run using 34% In grown (as an experiment) on a 2-micron thick graded buffer layer on an n^+ GaAs substrate (wafer InG 6-3, device run #55). Because of the large values of parasitic capacitance resulting from the n^+ substrate and the thin buffer layer, and because of velocity-degradation at the interface between the active layer and buffer layer, the rf performance was poor. However, measurements of the static characteristics yielded a saturation drift velocity of 1.8×10^7 cm/sec, or 40% higher than the value for GaAs.

One problem that was encountered was velocity degradation at the active layer-buffer layer interface. It was found that, by growing the last part of the buffer layer in the active layer growth position and lowering the growth rate so that no vapor etch was needed during the transition from buffer to active layer growth, the degradation at the interface could apparently be eliminated or at least minimized. In spite of velocity degradation at the interface and lower-

doped channels, InGaAs was able to match the performance of GaAs, which provides the basis for the expectation that once these problems have been eliminated and In percentages above 25% have been realized, InGaAs will significantly outperform GaAs.

The goal of this contract phase is to grow by VPE active layers of InGaAs having an In percentage of 25% and higher on linearly-graded buffer layers grown on semi-insulating GaAs substrates. Laser annealing and/or ion implantation are to be investigated as a means of eliminating built-in strain and interface states that give rise to velocity degradation at the active-buffer layer interface. FETs are to be fabricated on this material for the purposes of furthering material evaluation and to compare FET performance with that using GaAs at frequencies above 8 GHz.

2. MATERIAL GROWTH

Attempts at high percentage InAs in InGaAs growth in the present system using the same process as for lower InAs percentages required only the extension of the compositional grading program to higher percentages utilizing the composition versus In and Ga-HCl flow ratios from the literature.[14-16] A number of problems, however, appeared in growths for high InAs percentage. It was found that the surface quality deteriorated markedly for growths of >20% InAs concentration. The growth was found to be highly sensitive to substrate defects. Hillock-free growths were obtained only on low dislocation density substrates. All Cr-doped substrates from different sources such as Varian, Morgan Semiconductor, Monsanto, and Crystal Specialities showed highly degraded, dull gray, hazy surfaces. Figure 3 shows the surface of wafer InG 43-9 which has a dark blue hazy appearance which will be termed "blue haze." Excessive wall deposit buildup was also observed which could have interferred with the growth of high % InAs concentration on InGaAs.

In an attempt to improve the growth, slower grading rates (slower percentage In change per unit thickness) and smaller growth rates were attempted. The source temperature was reduced to about 800°C from 850°C used initially to reduce the growth rate, and the compositional grading program was extended after 15% In to allow for a slower grading rate. This procedure increased the total process time to over 4 hours for about 30% InAs in InGaAs growth which improved the quality of the growth greatly, but not without consequent depletion of the sources. However, a slightly bluish haze still persisted on the periphery of the 25-30% InAs wafers. The photoluminescence spectrum of the material

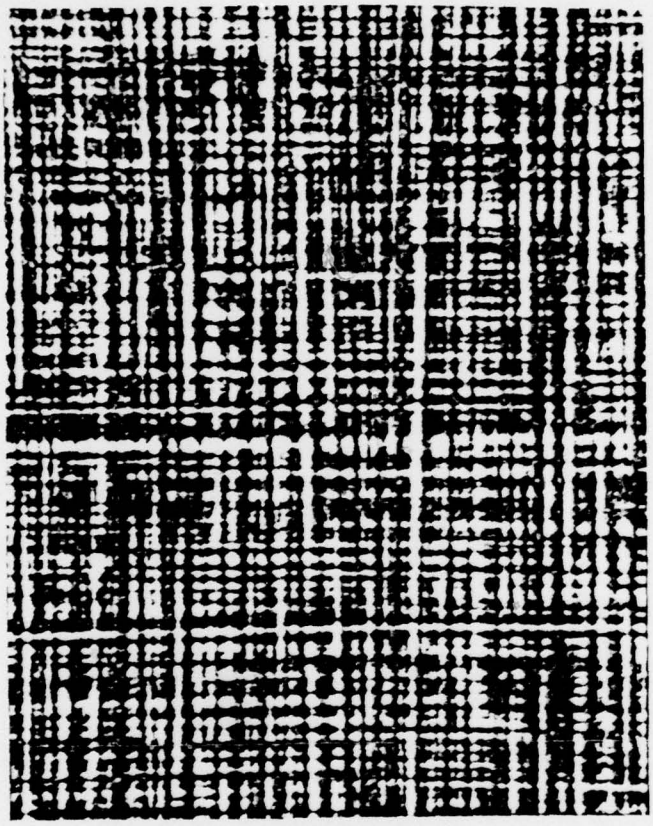

Fig. 3 Surface of wafer InG 43-9, illustrating what will be termed "blue haze".

also improved but was still not as narrow as that for material in the neighborhood of 18%. Figures 4 and 5 show a comparison of an 18% InAs and 25% InAs in InGaAs photoluminescence spectra. 25% InGaAs and 30% InGaAs material graded with Cr doping and with a ~$10^{17}cm^{-3}$ n-type active layer grown with this process were submitted for device fabrication (Section 4). Figure 6 and 7 show the doping profiles of these two wafers.

Figure 8 shows a cleaved and stained section of a wafer that showed surface haze. No gross growth defects that could have led to surface haze are seen in the section. Haze, if slight enough, can be removed by a short rinse in a light (< 0.1%) Br-Methanol solution. The photoluminescence spectrum, however, does not improve with the haze removal, indicating material deterioration near the surface. Auger sputter etch analysis of one such wafer having a dark haze seems to indicate a faster increase to high In percentage very near the surface, implying a faster grading rate due to reduced growth rate. This could be the cause of the hazy surface since reducing the grading rate by extending the programmed growth also seemed to improve the surface quality. Extending the programmed growth for high InAs percentage has its limits also in the present process as the extraneous wall deposits also increase with time. The growth rate at the wafer decreases because of competition with the wall deposits, effectively increasing the grading rate with time. Reducing the overall $AsCl_3$ mole fraction did not reduce the problem either. To avoid this problem, the wall deposits have to be avoided or reduced while maintaining a uniform grading rate. This can be accomplished by reducing the difference in temperature between the source and the substrate

Fig. 4
18% InGaAs photoluminescence spectra

Fig. 5 25% InGaAs photoluminescence spectra.

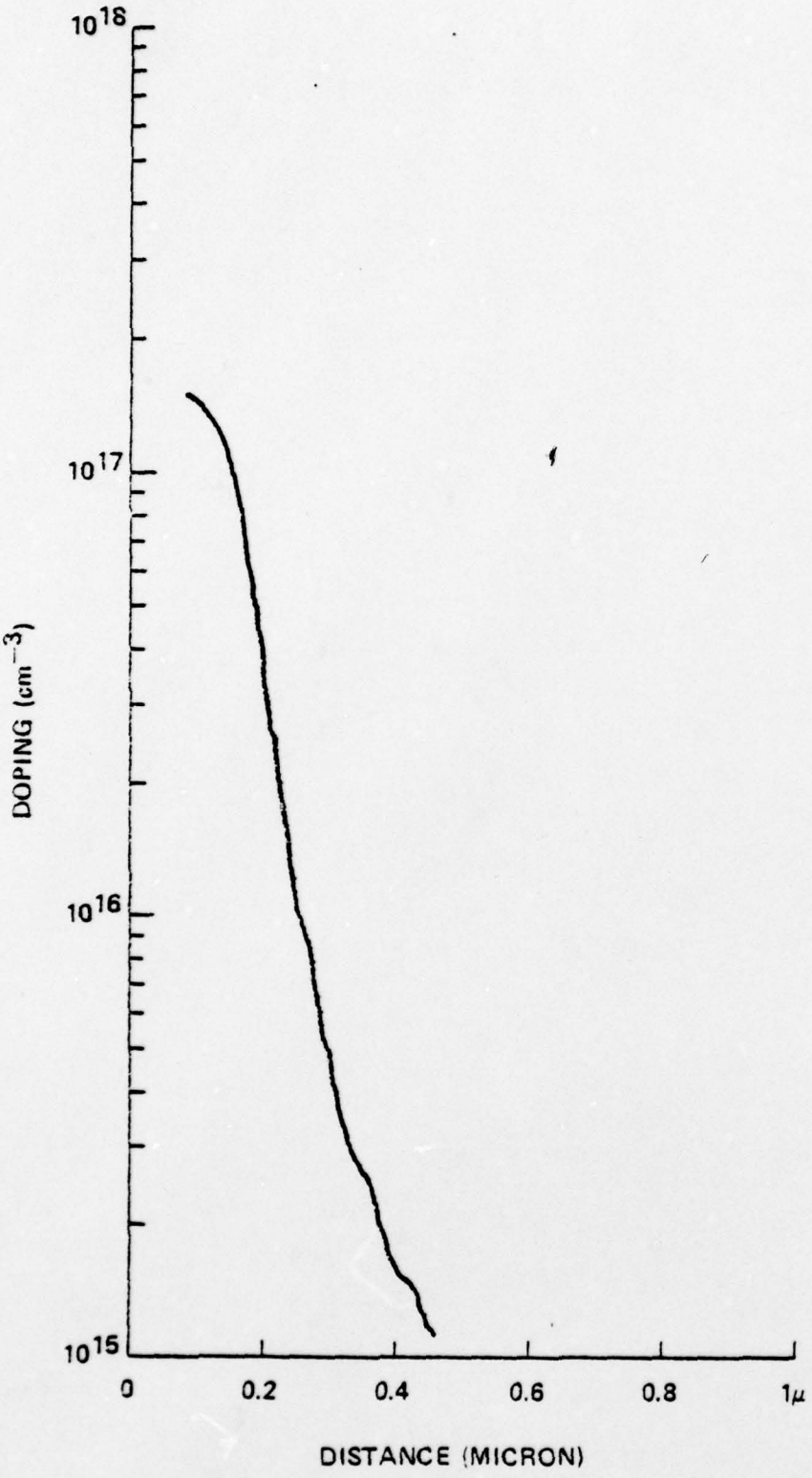

Fig. 6 25% InGaAs doping profile (wafer InG 37-9)

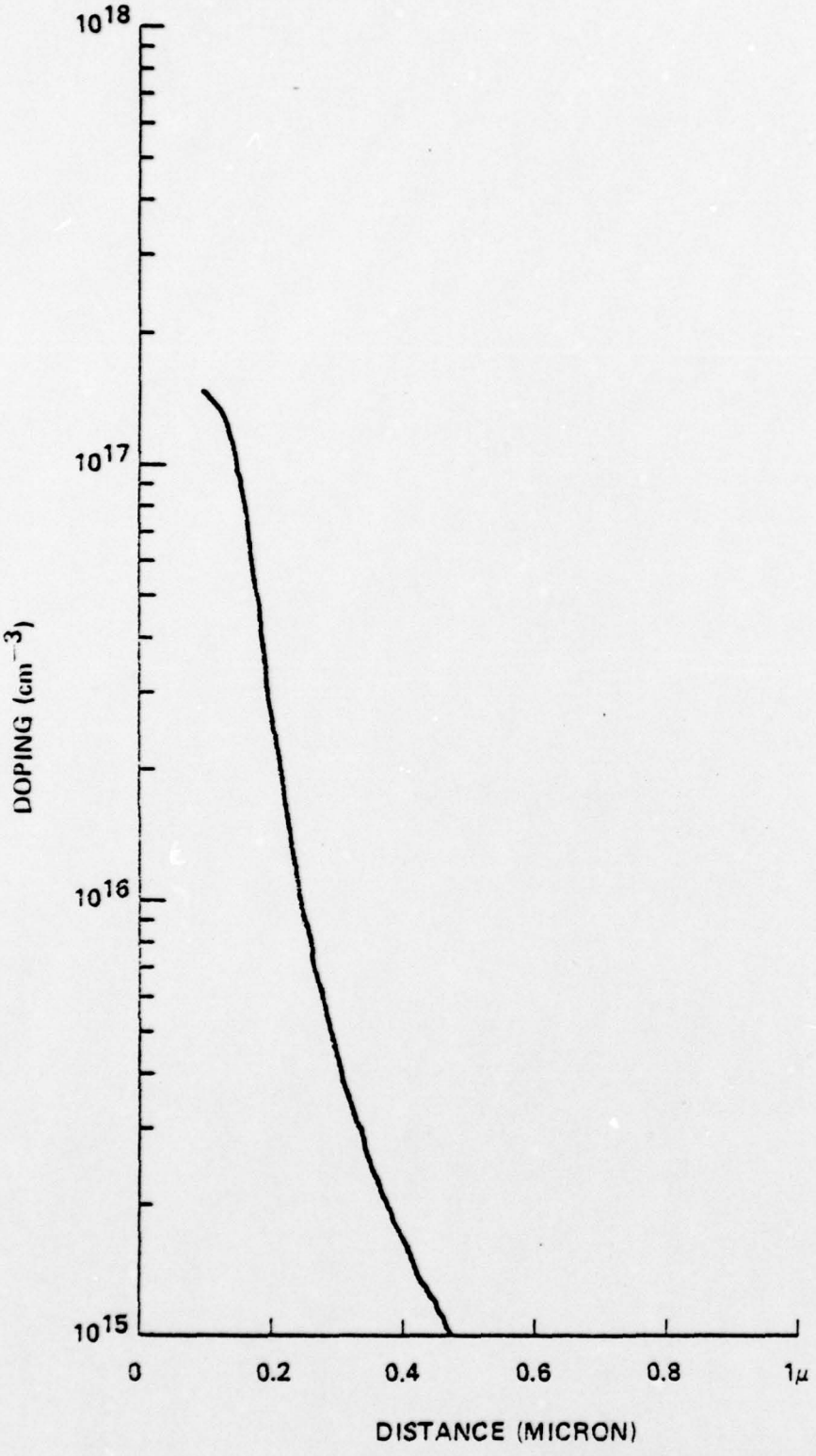

Fig. 7 30% InGaAs doping profile.
(wafer InG 37-11)

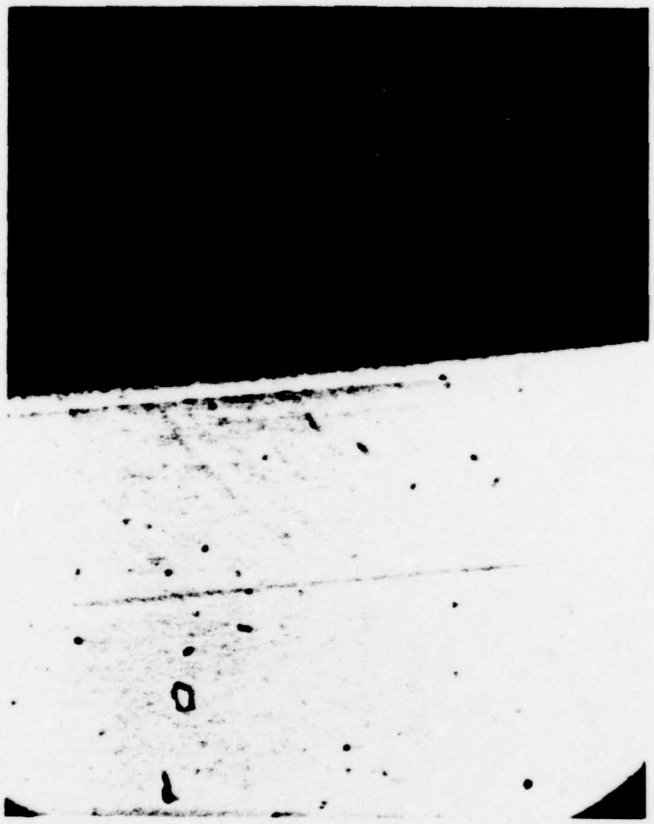

Fig. 8 Cleaved section of "blue haze" wafer

and decreasing the mole fraction of $AsCl_3$ over only the substrate by the use of an extra H_2 flow over the substrate, bypassing the source

Close to the end of this reporting period, a new reactor was fabricated incorporating the facility for bypass H_2 flow. A new flow controller was also added together with the assocaited controls to the original gas flow system. Figure 9 shows the new reactor system schematically. Capability of reactor etchback using cylinder HCl instead of $AsCl_3$ was also added. After preliminary growth and evaluation runs to establish proper growth conditions in the new reactor, graded layer growths to about 30% InAs concentration were grown with a bypass flow of 500 cc/min of H_2. An $AsCl_3$ bubbler temperature of 7°C was used together with a composition grading program extending over 15% to 30% InAs concentration ranges. Little or no bluish haze was observed in wafers grown with an H_2 bypass flow. The quality of growth seems to have improved also, as indicated by the photoluminescence spectrum of wafer InG 45-2 (29% In, 7.1 micron buffer layer grown on a Cr-doped (100) GaAs substrate of which 0.65 microns is constant composition, with no active layer) shown in Fig. 10. The half width is only 20 meV and the surface is one of the best seen so far with only a faint amount of cross-hatch. Wafer InG 46-1 (33% In, 10.7 micron buffer layer of which 1.1 micron is constant composition, with an active layer included) was also grown with the H_2 bypass and also had a surface with a minimum amount of cross-hatch with a photoluminescence half-width of 50 meV. Why the half-width is wider than for wafer InG 45-2 when the surface actually appears a little better is not clear. Of all the techniques tried in order to improve the surface quality, it appears that the H_2 bypass is the only one to significantly reduce the growth dislocations to acceptable levels.

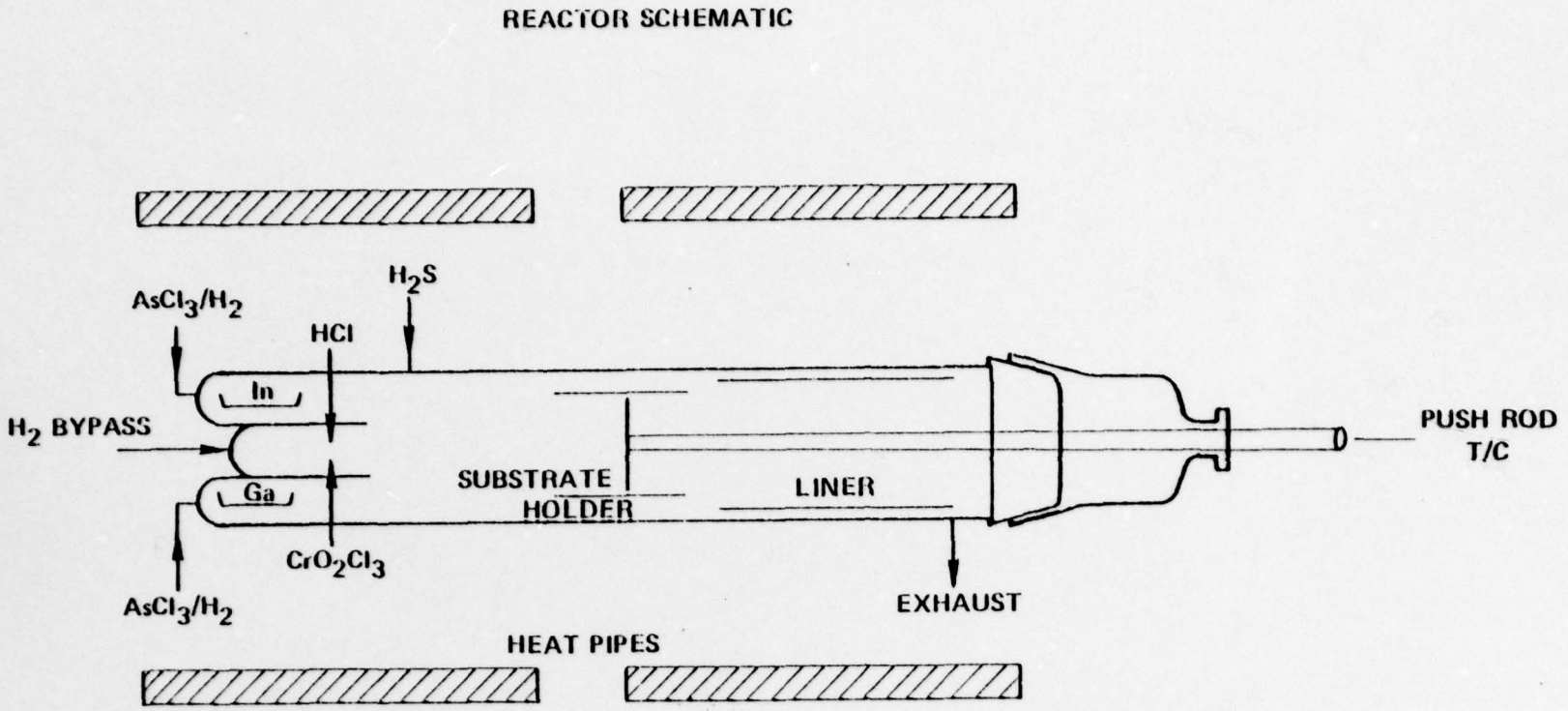

Fig. 9 Reactor system with H_2 bypass.

Fig. 10 Photoluminescence of H_2 bypass wafer InG 45-2.

3. ION IMPLANTATION AND LASER ANNEALING

3.1 Ion Implantation of InGaAs

Two of the InGaAs Cr-doped buffer layer wafers grown for ion-implantation were given a Si implant at 100 keV. The dose was $2 \times 10^{-12} cm^{-2}$ and the implant was done at room temperature. Both wafers had an In percentage above 30% and hence had the "blue haze" problem spoken of in Sec. 2. Prior to implantation the wafers were given a light Br-Methanol polish to produce a mirror finish on the surface.[17]

Wafer InG 32-3 (~35% In, with the buffer layer greater than 6 microns, 1.5 microns or more of which is constant composition) had its "blue haze" polished off and was implanted. After the implantation the surface was still mirror-like in appearance. A Si_3N_4 cap was then put down on the surface at 200°C by plasma deposition (having an index of refraction of 2.0) and the wafer was thermally annealed at 800°C for 30 min. After the nitride was removed, the surface was no longer mirror smooth, having a "cream-of-wheat" texture to it as shown in Fig. 11. Au dots were deposited on the surface for purposes of obtaining a doping profile, but shunt leakage prevented this even to the point of not being able to determine the capacitance at zero bias. The I-V characteristics of the dots showed rectification, with the reverse characteristic suggesting the presence of a large number of generation-recombination centers in the depletion region of the Schottky barrier.

The identical procedure used for wafer InG 32-3 was repeated for wafer InG 32-7 (~34% In, with the buffer layer

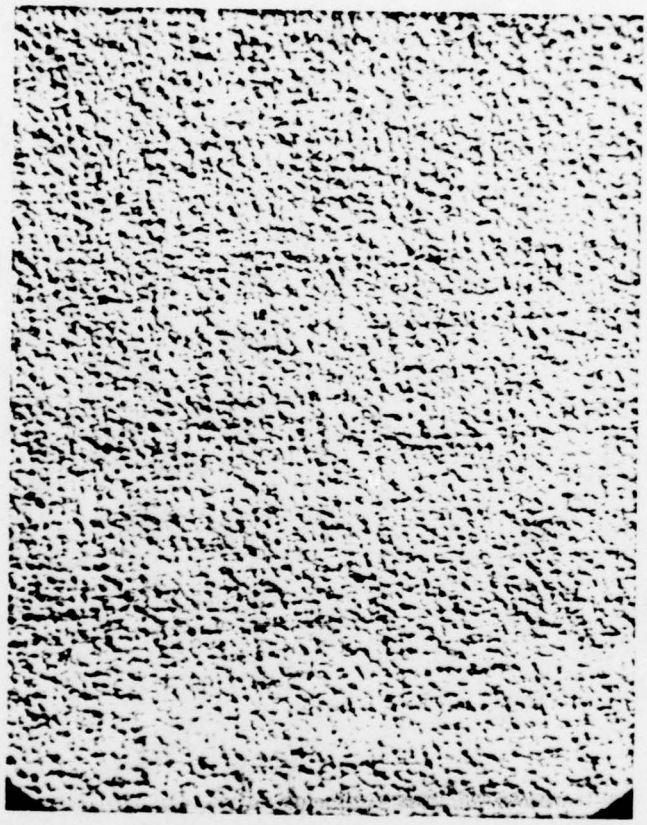

Fig. 11 Surface texture of wafer InG 32-7 after thermal anneal at 800°C for 30 min.

greater than 6 microns, 1.5 microns of which is constant composition) with almost identical results. After the surface polish removing the "blue haze", the surface retained a small amount of cross-hatch which converted to the "cream-of-wheat" surface shown in Fig. 11. Au dots were ohmic with no hint of rectification.

Figure 11 is actually of wafer InG 32-7, with the surface of InG 32-3 showing the same texturing effect but to a lesser degree. While Fig. 3 was taken without the use of phase contrast, phase contrast was needed for Fig. 11 in order to plainly see the surface texture. Thus, although the surface deteriorates during the anneal cycle, it does not approach the "blue haze" condition it had prior to the Br-Methanol polish. The better surface of InG 32-3 may be related to its better I-V characteristics, signifying a connection between the optical appearance of a wafer and its electrical properties.

Photoluminescence of both wafers revealed absolutely no response whatsoever, presumably indicating no activation of the implanted species. No photoluminescence data was taken on the wafers after growth since Cr-doped material typically shows no response.

In order to determine if the problem of surface deterioration with anneal is related to the initial "blue haze" surface of the wafer, the identical implantation and anneal process was done on wafers having an In percentage below 20% and which, consequently, did not have the blue haze problem. Wafer InG 36-10 (17% In, ~3 micron graded buffer layer with 0.5 micron of constant composition followed by an active

layer) and wafer InG 36-16 (8% In, ~4 micron graded buffer layer) were first covered with nitride and annealed at 800°C (no implant) to see if the surface would deteriorate as for the 34 and 35% In wafers. The surfaces remained the same, as did also the photoluminescence spectra (except for a slight broadening on one side of the peak). The active layer was polished off wafer InG 36-10 and both wafers were given the same implant as the 34 and 35% In wafers, after which they were capped and annealed. The surfaces did not deteriorate, but photoluminescence revealed an added peak for wafer InG 36-10 (Fig. 12) and an added hump to the peak of wafer InG 36-16 (Fig. 13). The added peak may be a defect peak resulting from the implantation and anneal processes. The photoluminescence data also revealed that the In percentage for wafer InG 36-10 was reduced to 10% from its original value of 17%, evidently because of the material removed when the active layer was polished off. Either more material was removed than intended or, as suggested by the Auger profile mentioned in Sec. 2, most of the In change occurs in the last part of the growth rather than as programmed. Figures 14 and 15 give the implanted doping profiles of the two wafers. These wafers were not processed into devices because the In percentage was so low.

In summary, the difficulty in activation of the implanted species and surface deterioration during anneal was not seen for wafers having an In percentage less than 20%. Whether these difficulties are encountered with the higher In percentages because of the "blue haze" or as an intrinsic result of the higher In percentage is not known at this time. The deterioration of the surface during the anneal after the blue haze has been polished off seems to suggest that the

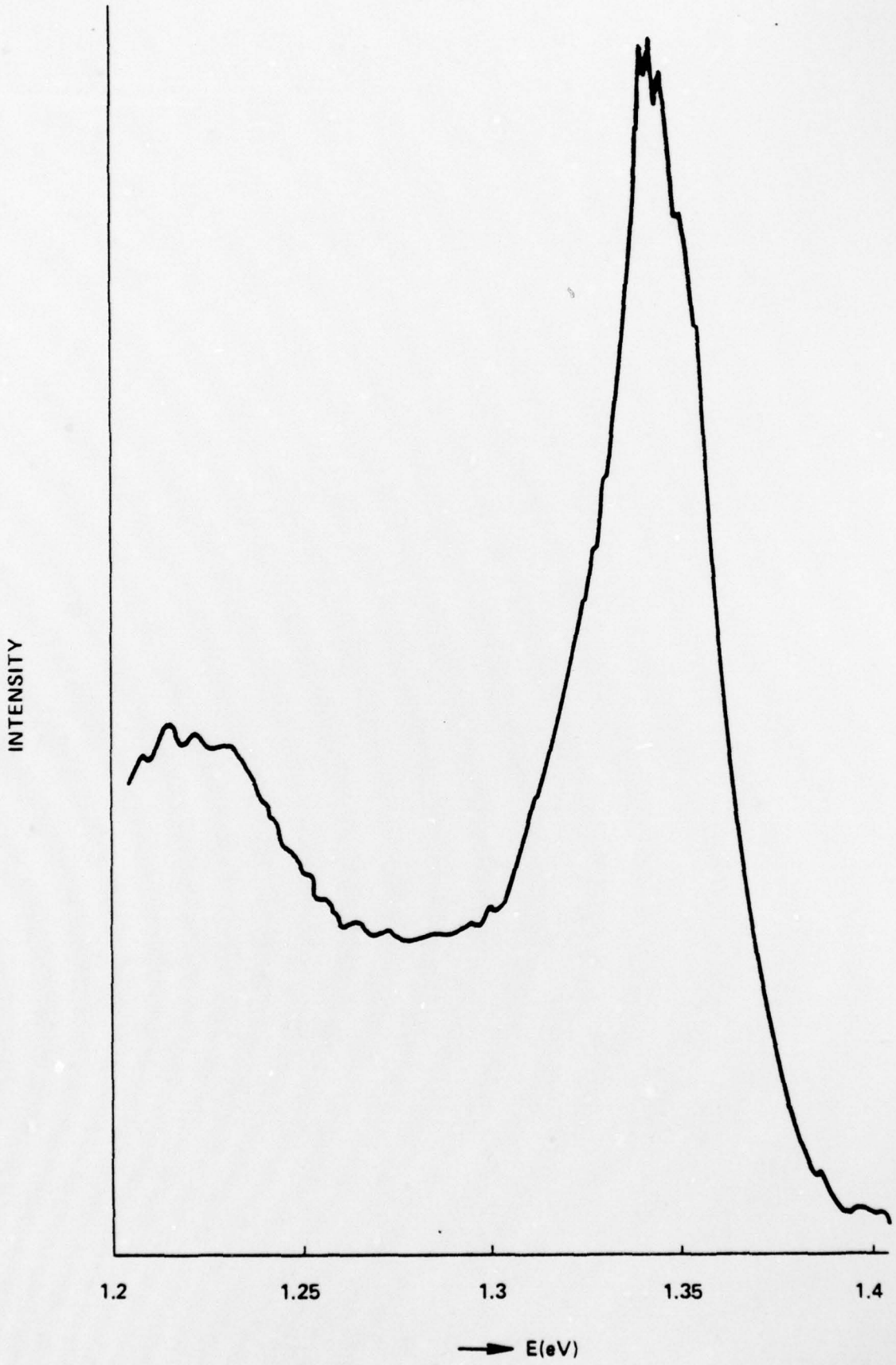

Fig. 12 Photoluminescence of annealed wafer InG 36-10.

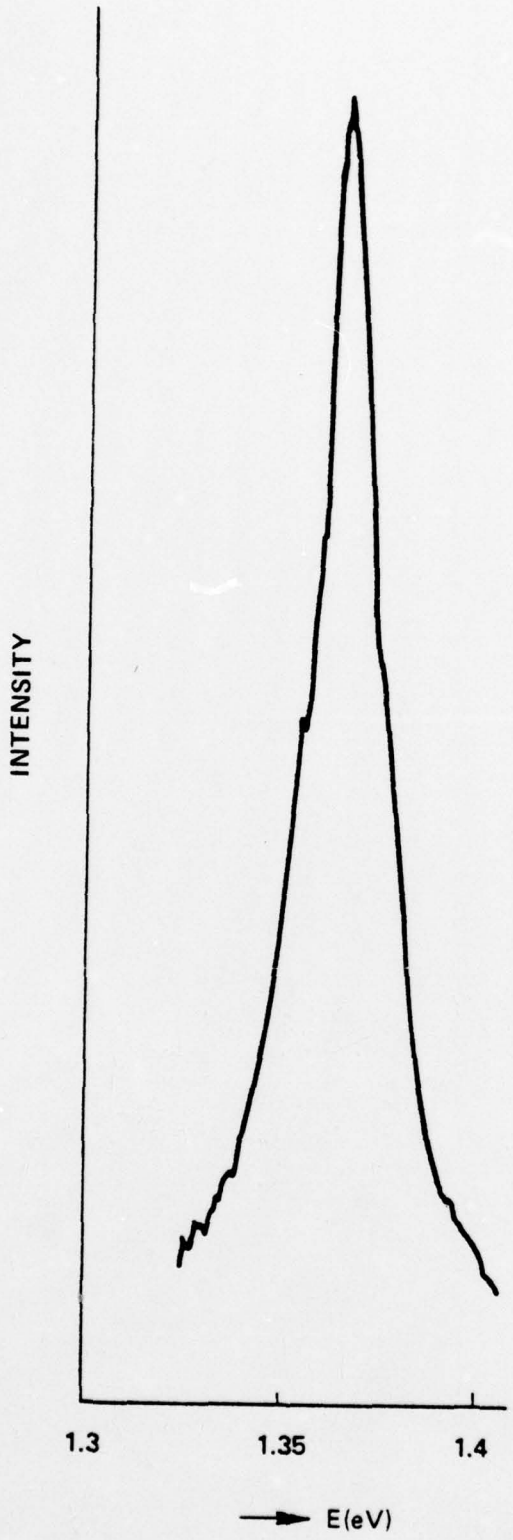

Fig. 13 Photoluminescence of annealed wafer InG 36-16.

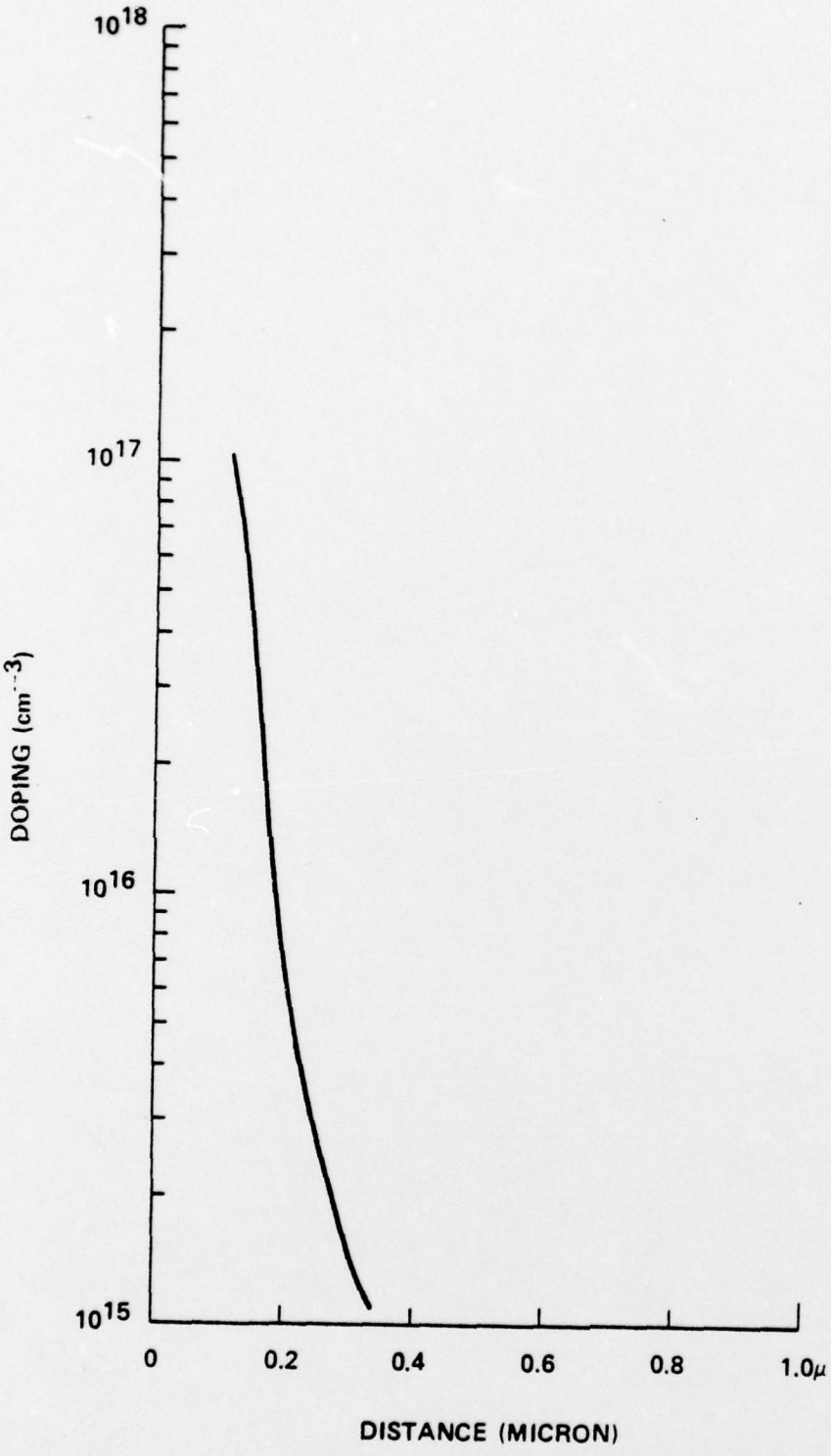

Fig. 14 Implanted doping profile of wafer InG 36-10.

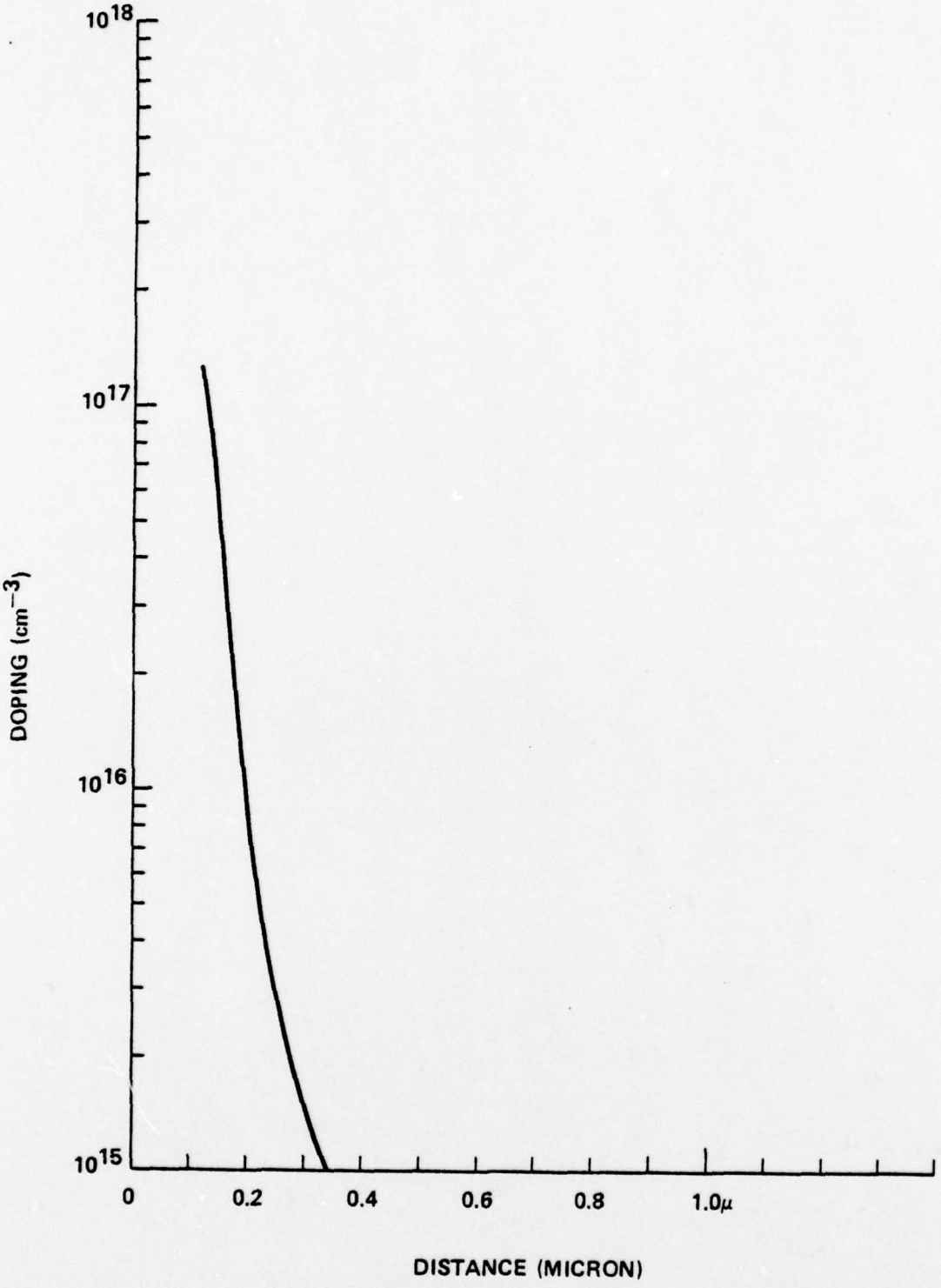

Fig. 15 Implanted doping profile of wafer InG 36-16.

blue haze is not just a surface phenomenon as originally thought, but is indicative of the nature of the underlying material.

3.2 Laser Annealing

Using a Q-switched ruby laser with pulse lengths of 25-40 ns, no electrical activation of Si was seen in 100 keV Si-implanted Cr-doped GaAs with doses less than $1 \times 10^{14} cm^{-2}$. Table I shows the electrical activation and mobility of uncapped GaAs with 100 keV Si implant doses of $1 \times 10^{14} cm^{-2}$.

TABLE I

SUMMARY OF GaAs LASER ANNEAL RESULTS

Laser Energy	Pulse Duration	Carrier Concentration	Mobility
1.1 J/cm^2	40 nsec	$8.1 \times 10^{12} cm^{-2}$	680 $cm^2/V\text{-}sec$
1.1	25	2.2×10^{13}	600
1.3	30	6.4×10^{13}	330
1.8	25	2.6×10^{13}	300
800°C thermal anneal	30 min.	2.4×10^{13}	2330

This data indicates a reduction of mobility with increasing laser energy, with the maximum value being only 30% of the value obtained by thermal annealing. The data suggests that perhaps higher mobilities can be obtained by reducing the beam energy below 1.1 J/cm^2, but at the expense of reducing the carrier activation to even less than the 10% value of 1.1 J/cm^2. No improvement was seen using a nitride cap

during the anneal and, in fact, the best mobilities were obtained without the nitride cap (most of the time the nitride cap would blow off). The data in Table I agrees with the results of others using Q-switched laser annealing as reported in the literature. The laser energy threshold for salient surface decomposition to occur was found to be 1.5 J/cm^2.

Using the laser in the free-running mode without the Pockel cell (0.2 ms pulses), no electrical activation of the Si-implanted GaAs was seen for energies all the way up to 2.8 J/cm^2.

Laser annealing was investigated not only for purposes of annealing out ion implantation damage without significant dopant diffusion, but also as a possible means of eliminating built-in lattice strain encountered in growth (which manifests itself in surface quality typified by cross-hatching and "blue haze" as shown in Fig. 3) and to reduce interface strain or states between the active and semi-insulating buffer layers (which is presumed to cause the saturated velocity degradation encountered in previously fabricated InGaAs FETs[1]). Laser annealing will permit approaching the melting temperature for very short periods of times to hopefully reduce the strain in the same manner that it is used to recrystallize amorphous deposited layers.[18] The low mobilities in Table I indicate that the laser is incapable of removing all of the lattice damage, and the hazy surfaces such as shown in Fig. 3 are sure to reflect the incident beam to a varying degree so that the net incident energy cannot be controlled. Consequently, laser annealing of the InGaAs wafers to see if the cross-hatch or blue haze evident on the surface could be removed was not tried. Electron-

beam annealing[19] is much more controllable in that the energy and time can be varied independently and over a wider range in addition to eliminating the reflection problem. Varian is in the process of developing a capability to electron-beam anneal, and the intention is to use this process on the InGaAs wafers, depending upon its results with GaAs.

4. DEVICE FABRICATION AND EVALUATION

FETs were fabricated on five of the best wafers grown during this period. Two of the wafers were 30% In grown at the same time on Cr- and Te-doped substrates with a 15.7-micron thick buffer layer. Both wafers, although having slightly hazy surfaces, were the least hazy of all the wafers grown having an In content above 25%. Another two of the wafers were 22% In grown at the same time on Cr- and Te-doped substrates with a 17-micron buffer layer (having shiny surfaces but with a pronounced amount of cross-hatch) and the remaining wafer was 25% In grown on a Cr-doped substrate with a 14-micron buffer layer (having the least amount of cross-hatch of all the wafers but with growth hillocks all over the surface). The buffer layers on all of these wafers were linearly graded with no constant composition layers (the blue haze phenomenon was independent of whether or not a constant composition layer was included in the growth of the buffer layer). The photoluminescence peak half-width was about the same for all three In percentages, ranging from 28 to 35 meV.

The FET device geometry used is shown in Fig. 16. The gate width Z is 150 microns and the length L is in the 0.5 to 1.0-micron range. The gates were defined by electron beam exposure of PMMA resist and consist of 1000 Å of sputtered Pt overlaid with around 3000 Å of evaporated Au. Au-Ge/Ni/Au was used for the ohmic contacts. The fabrication sequence in order was: mesa etch, ohmic contact formation, gate deposition, and Au overlay.

Table II summarizes the results of the device runs, with Figs. 17-19 giving the drain characteristics of a

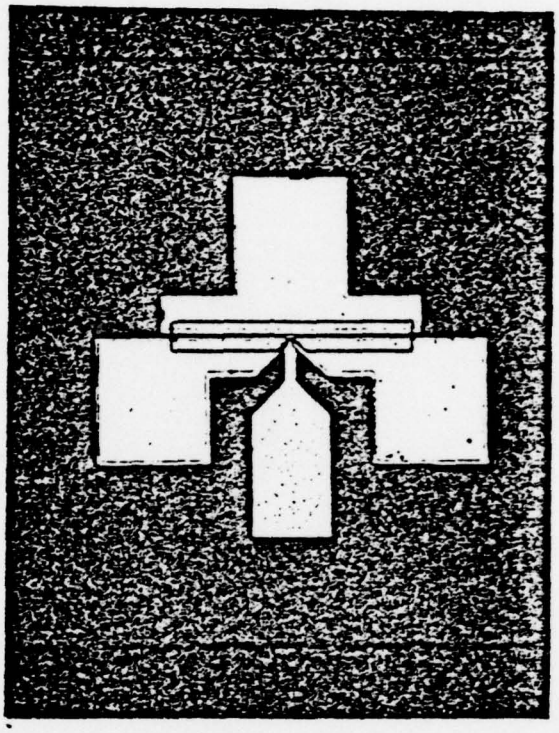

Fig. 16 Device geometry used for InGaAs FETs

device from each of the runs. Appendix A outlines the technique of determining the effective saturated drift velocity v_s from the drain characteristic of the devices. Based on this analysis, the effective saturated drift velocities given in Table II were computed from the plots shown in Fig. 20, which in turn were derived from the drain characteristics of Figs. 17-19 using the barrier height ϕ_B given in Ref. 20. When the technique of Appendix A is applied to GaAs, a value of 1.3×10^7 cm/sec is typically found, while when applied to the 34% In run described in Section 1, a value of 1.8×10^7 cm/sec was obtained. Evidently the pronounced cross-hatch of the 22% wafers and the blue haze of the 30% wafers prevented v_s from even reaching its GaAs value.

Appendix B gives the s- and y-parameters for all of the runs along with the power gains computed from them.

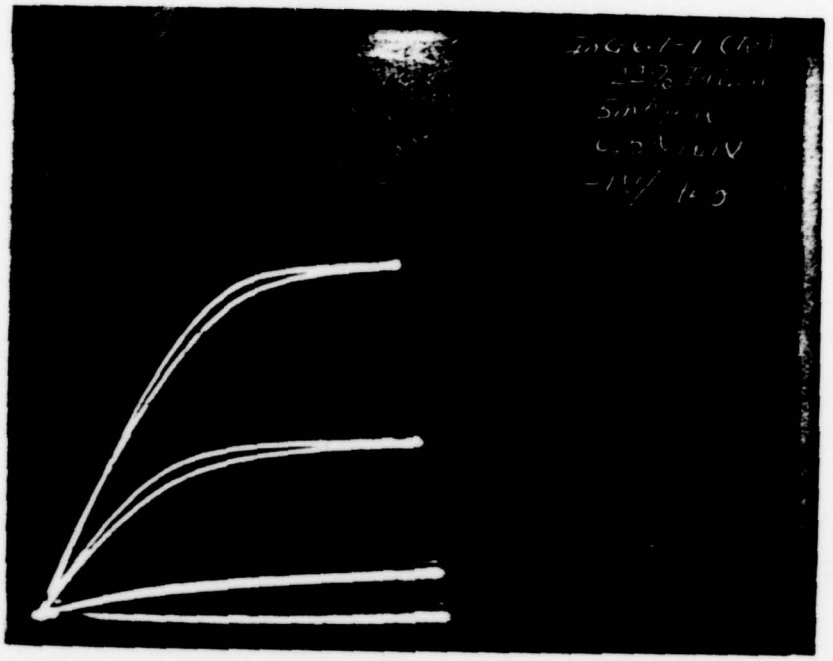

Fig. 17 Drain characteristics of a device from run 67 (22% In).

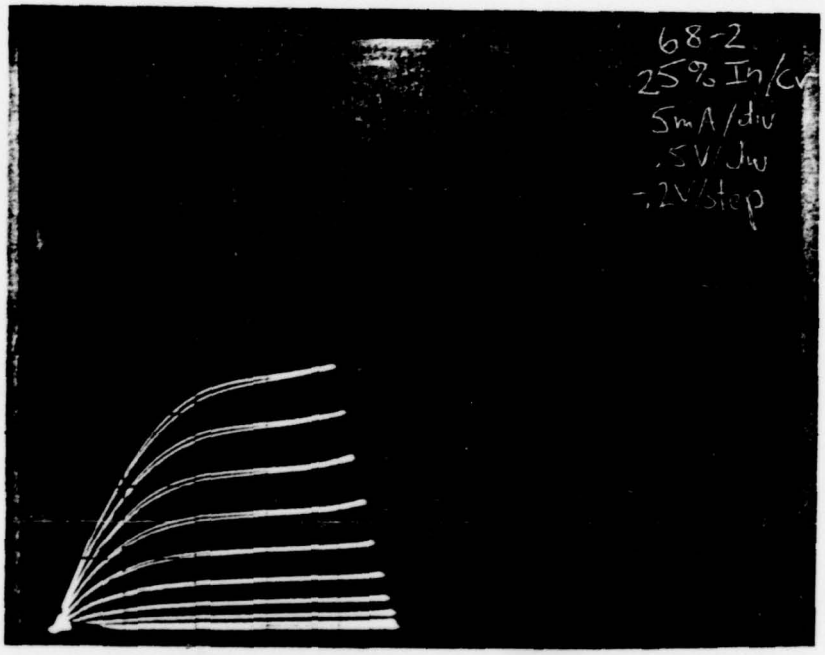

Fig. 13 Drain characteristic of a device from run 68 (25% In).

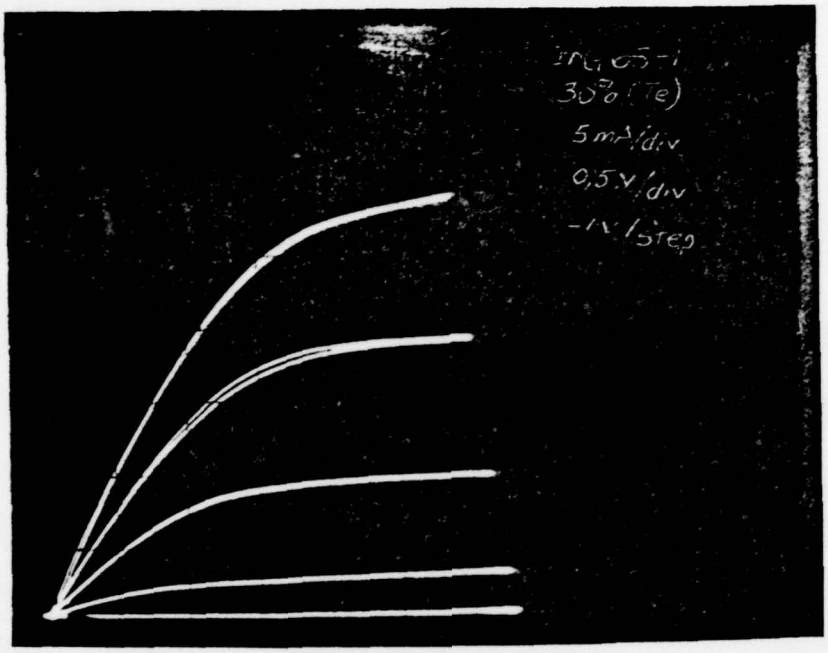

Fig. 19 Drain characteristic of a device from run 65 (30% In).

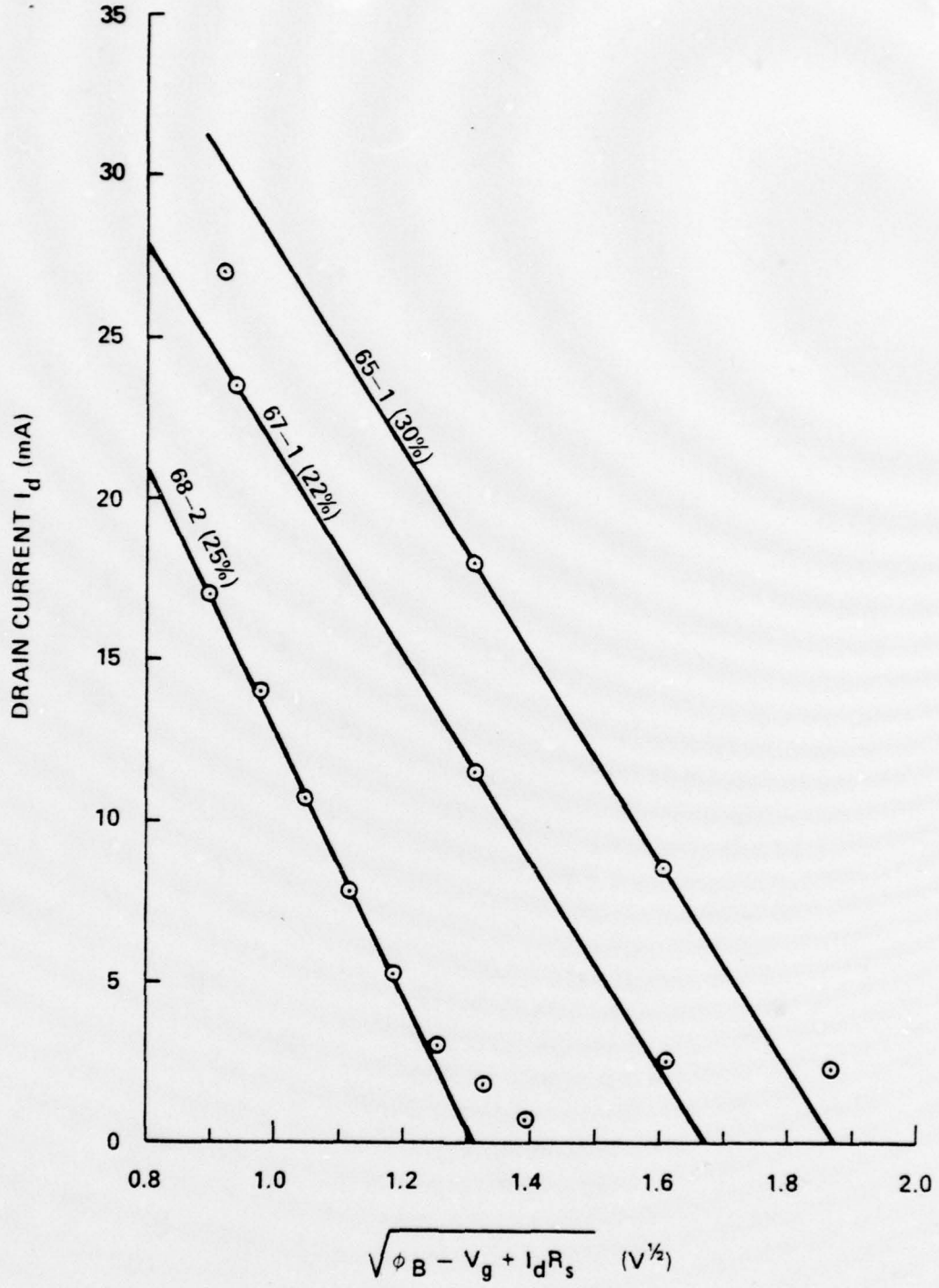

Fig. 20 Application of Appendix A technique to devices of Figs. 17-19.

TABLE II

SUMMARY OF InGaS FET RESULTS

Run	%In	N_d (cm^{-3})	v_s (cm/sec)	MAG (dB) at 8 GHz	NF_m (dB) at 8 GHz	G_a (dB) at 8 GHz
64	30% on Cr-doped substrate	1.5×10^{17}	$< 9.8 \times 10^6$	15-17		
65	30% on Te-doped substrate	1.5×10^{17}	9.8×10^6			
66	22% on Cr-doped substrate	2.0×10^{17}	$< 9.0 \times 10^6$			
67	22% on Te-doped substrate	2.0×10^{17}	9.0×10^6			
68	25% on Cr-doped substrate	1.5×10^{17}	1.26×10^7	15	3.57	13

5. CONCLUSIONS AND RECOMMENDATIONS

It has been found that for InGaAs growths with an In percentage at and above 25% the surface appears to have what is termed "blue haze", which results from a crosshatch pattern of defects. This blue haze begins to appear at around 25% In and becomes progressively worse as the In percentage is increased. Photoluminescence peaks of the surface layers begin broadening at 25% and continue to broaden as the In percentage is increased. Although the blue haze can be polished off, leaving a mirror finish, there is evidence that it is indicative of the nature of the underlying material. FETs fabricated on this material have smaller effective saturated drift velocities than for GaAs, as well as inferior rf performance. Ion implantation of this material was unsuccessful.

Almost all of the effort on this contract this past year was spent in trying to overcome the "blue haze" problem. It was felt that the problem was not intrinsically associated with the higher In percentages, since the 34% In growth of the previous contract had no such problem. The intention was to duplicate the good growth obtained for that 34% In growth (grown in an earlier version of the reactor using only a 2-micron buffer layer). Many techniques and substrates were tried with limited or no success and it was not until at the very last of this contract phase when an H_2 bypass was was installed on the reactor that haze-free surfaces were obtained. Two wafers having surfaces with a minimum of cross-hatch have been grown with the H_2 bypass, and FETs will be fabricated on them for purposes of evaluation. It might also be interesting to electron-beam anneal the blue haze wafers to see if the dislocation network can be removed.

6. PROPOSAL FOR FUTURE WORK

Other work at Varian has shown that $In_{0.53}Ga_{0.47}As$ alloys can be grown by liquid phase epitaxy, lattice matched on InP, with mobilities in the region of 8000 cm^2/V-sec at 300°K, for dopings of $10^{17}/cm^3$, or nearly twice that for comparable GaAs. (For convenience, the specific lattice-matched $In_{0.53}Ga_{0.47}As$ alloy will be abbreviated as InGaAs in what follows.) The mobility increase is to be expected from the reduced bandgap, but the result indicates that alloy scattering is low in this alloy. Figures 21 and 22 show plots for the entire range of quaternaries from InP to InGaAs of mobility, Schottky-barrier height, and estimated satellite valley spacing (Γ - L; X appears to lie higher than L for the entire range of alloys matched to InP). The high mobility of InGaAs is coupled with a large (1.0 eV) gap to the nearest conduction band satellite valley. This implies that under the moderately high fields found in a microwave FET, considerable velocities can be reached in the central Γ valley before transfer to the L satellites sets in. To achieve this in GaAs requires the use of strong "overshoot" effects, i.e. gate lengths in the region of 0.1 μm.[21] However, the overshoot effect should be seen for more conventional dimensions (0.5 to 1 micron) in InGaAs. A transition to still shorter gate lengths using InGaAs should, of course, maintain the advantage over GaAs.

Some concern remains regarding the possibility of low-field avalanching in a material where the bandgap (0.73 eV at 300°K) is less than the satellite valley spacing (about 1.0 eV for Γ - L). However, this does not appear to be troublesome. Experiments in this laboratory with high-field bias-assisted photoemission from InGaAs[22] show that fields

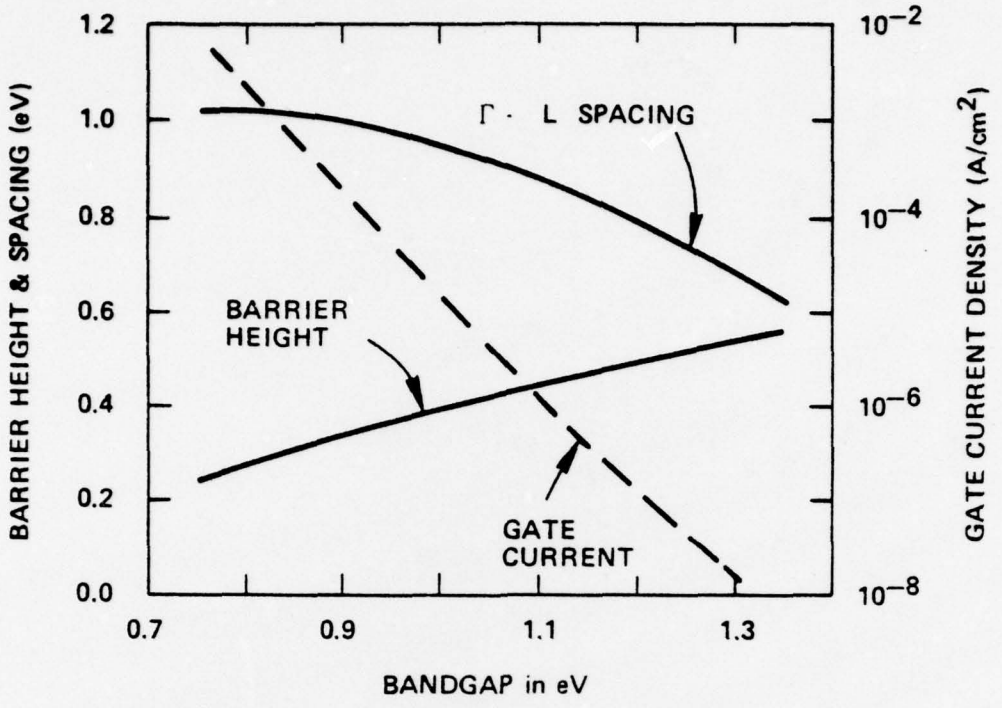

FIGURE 21

Quaternary barrier height, Γ-L spacing, and leakage current as a function of bandgap.

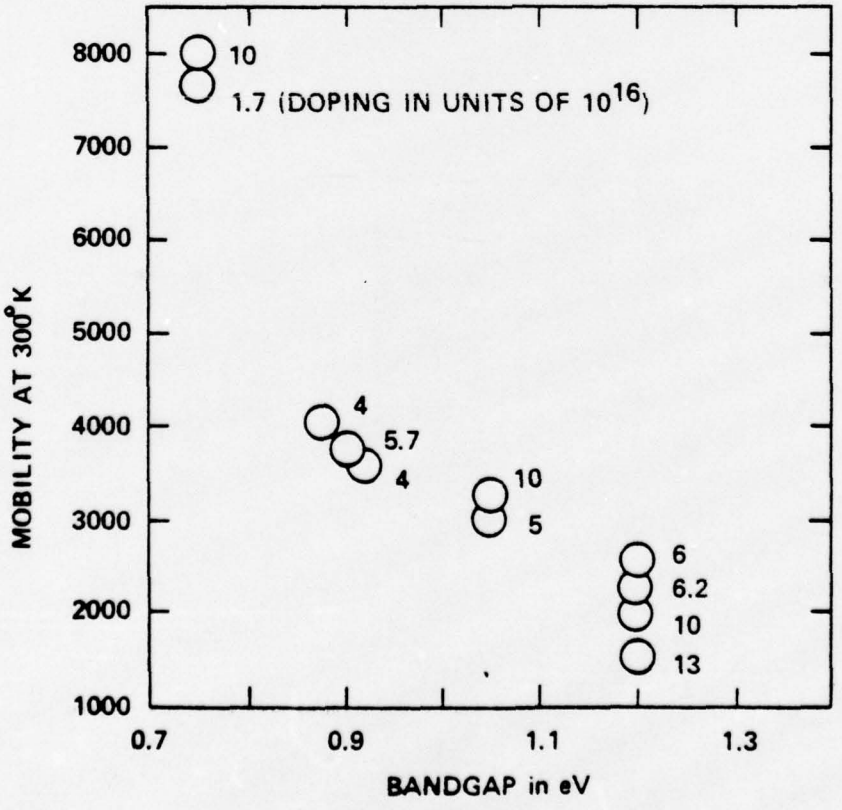

FIGURE 22

Experimental mobilities as a function of quaternary bandgap.

adequate for Γ - L transfer can be applied without avalanching. Once transfer to the heavy-mass L and X-band edges is achieved, a very large further increase in field is necessary to produce significant electron-hole pair generation. Fields used in the photoemission experiments[22] are of the order of 30 kV/cm. Qualitatively, InGaAs would be expected to behave somewhat like GaSb, which has a direct gap of about the same magnitude. Computations of Hauser[22] show that fields of about 200 kV/cm would be required in 10^{17}-doped GaSb to cause avalanching.

As can be seen from Fig. 21, the low Schottky-barrier height on InGaAs leads to very high gate current densities, and indeed initial attempts to fabricate MESFETs directly on this alloy at Varian have led to shorted gates. At the same time, attempts to use oxides or other insulators on III-V compounds have met with very limited success, due to high densities of interface states and instabilities of the insulators themselves. Accordingly, we propose the use of lattice-matched InP or the higher bandgap InGaAsP quaternaries:

(1) in n-type form to provide the higher Schottky-barrier (Figs. 23a and 23b), or
(2) in p-form to provide a junction FET (Fig. 23c).

In either case, the channel electrons flow in the low-bandgap high-mobility material, while the adjacent high-bandgap material is depleted; hence the low mobility of the depleted material is of no consequence. Figure 23b has an advantage over 23a in that ohmic source and drain contacts to the InGaAs should be easier. This may not be a very significant advantage, considering the extra complexity.

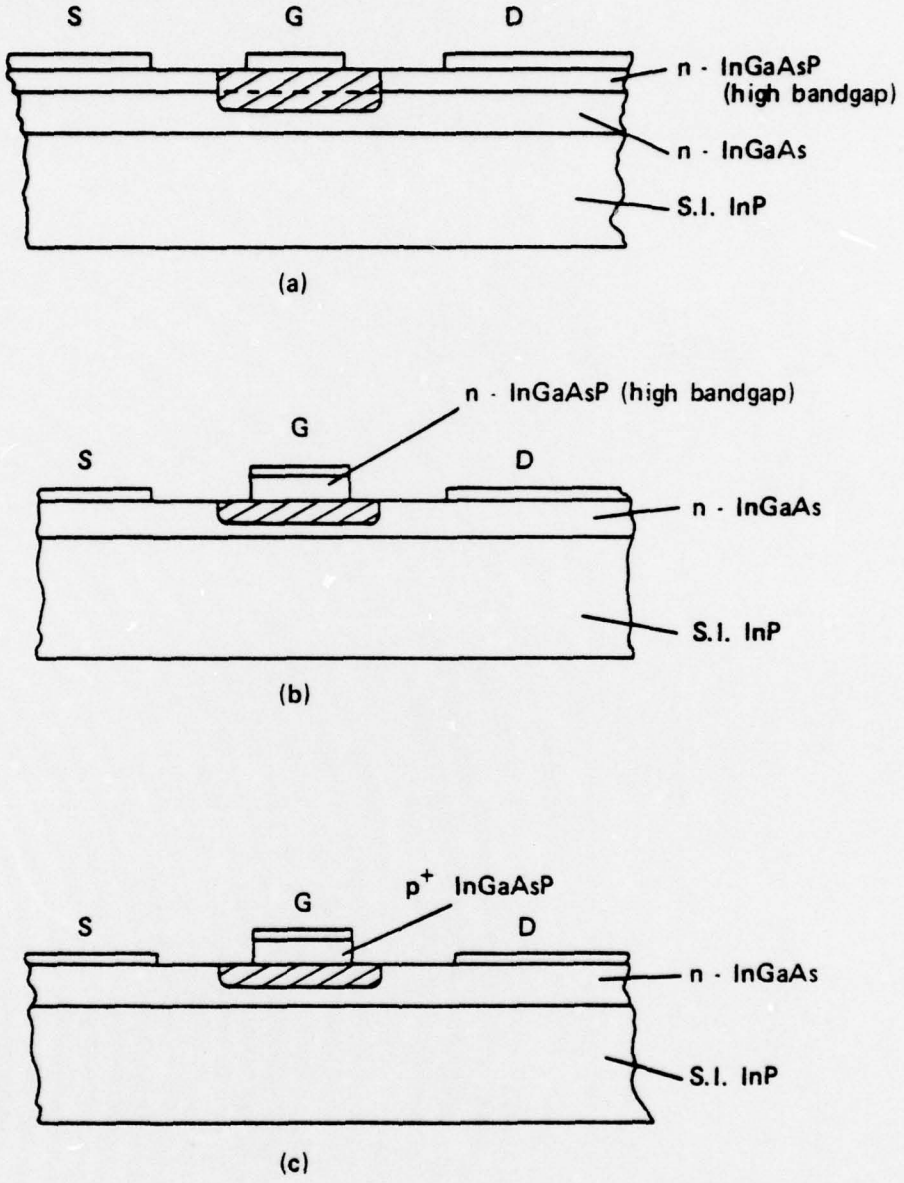

FIG. 23 Possible Gate Configurations for InGaAs FET.

The junction FET of Fig. 23c has the advantage of a still higher barrier height, if diffusion of the acceptor species in the p gate can be adequately controlled. A low-resistance gate contact can be developed using Be implantation.

Initial work would use LPE growth of the layers, which has given the highest mobilities in InGaAs. Experimentally, it has been found easier to grow high-bandgap quaternaries on InGaAs than pure InP on InGaAs. In all cases, very thin layers are needed, especially for submicron devices, providing strong motivation for development of complete vapor phase growth of these systems. Vapor phase growth of InGaAs on InP has not yet demonstrated the high mobilities of LPE. However, this work is in a very preliminary stage, and we would propose to devote some effort to improving the state of VPE of InGaAs grown on InP for this application. Ultimately, MBE may be applicable to the proposed structures. However, MBE technology has far to go in this area, and meanwhile feasibility investigations can be carried out using more conventional growth techniques. The use of different materials for gate and channel also suggests the applications of selective etching for submicron self-aligned structures.[24]

7. REFERENCES

1. S. G. Bandy, S. B. Hyder, T. J. Boyle, and C. K. Nishimoto, "InGaAs Microwave FET," Final Report, N00014-75-C-0125, Office of Naval Research, Arlington, VA (August 1979).

2. J. G. Ruch and W. Fawcett, "Temperature Dependence of the Transport Properties of Gallium Arsenide Determined by a Monte Carlo Method," J. Appl. Phys. 41, 3843 (1970).

3. J. G. Ruch, "Electron Dynamics in Short Channel Field-Effect Transistors," IEEE Trans. ED-19, 652 (1972).

4. T. J. Maloney and J. Frey, "Transient and Steady-State Electron Transport Properties of GaAs and InP," J. Appl. Phys. 48, 781 (1977).

5. W. Fawcett and D. C. Herbert, "High-Field Transport in Gallium Arsenide and Indium Phosphide," J. Phys. C: Solid State Phys. 7, 1641 (1974).

6. A. R. Adams, P. J. Vinson, C. Pickering, G. D. Pitt, and W. Fawcett, "3-Level Conduction-Band Structure of GaAs from High-Stress and High-Field Measurements," Electron. Lett. 13, 46 (1977).

7. D. C. Herbert, W. Fawcett, and C. Hilsum, "High-Field Transport in Indium Phosphide," J. Phys. C: Solid State Phys. 9, 3969 (1976).

8. J. C. Woolley, C. M. Gillet, and J. A. Evans, "Electrical and Optical Properties of GaAs-InAs Alloys," Proc. Phys. Soc. 77, 700 (1961).

9. R. E. Nahory, M. A. Pollack, and J. C. DeWinter, "Growth and Characterization of Liquid-Phase Epitaxial $In_xGa_{1-x}As$," J. Appl. Phys. 46, 775 (1975).

10. D. E. Aspnes, "GaAs Lower Conduction-Band Minima: Ordering and Properties," Phys. Rev. B 14, 5331 (1976).

11. J. R. Chelikowsky and M. L. Cohen, "Nonlocal Pseudopotential Calculations for the Electronic Structure of Eleven Diamond and Zinc-Blende Semiconductors," Phys. Rev. B 14, 556 (1976).

12. E. O. Kane, "Band Structure of Indium Antimonide," J. Phys. Chem. Solids 1, 249 (1957).

13. W. Fawcett, C. Hilsum, and H. D. Rees, "Optimum Semiconductor for Microwave Devices," Electron. Lett. 5, 313 (1969).

14. R. E. Enstrom, D. Richman, M. S. Abrahams, J. R. Appert, D. G. Fisher, A. H. Sommer, and B. F. Williams, "Vapor Growth of $Ga_{1-x}In_xAs$ Alloys for Infrared Photocathode Applications," in Proc. Third International Symposium on Gallium Arsenide and Related Compounds, ed., K. Paulus (Institute of Physics, London, 1971), p. 30.

15. R. W. Conrad, P. L. Hoyt, and D. D. Martin, "Preparation of Epitaxial $Ga_xIn_{1-x}As$," J. Electrochem. Soc. 114, 164 (1967).

16. V. S. Van and M. Ettenberg, "Mass Spectrometric and Thermodynamic Studies of CVD of $In_{1-x}Ga_xAs$," in Chemical Vapor Deposition, Fourth International Conference, eds. G. F. Wakefield and J. M. Blocher, Jr. (The Electrochemical Soc., Inc., Princeton, NJ, 1973), p. 31.

17. G. H. Olsen, M. S. Abrahams, and T. J. Zamerowski, "Asymmetric Cracking in III-V Compounds," J. Electrochem. Soc. 121, 1650 (1974).

18. S. S. Lau, W. F. Tseng, M-A. Nicolet, J. W. Mayer, R. C. Eckardt, and R. J. Wagner, "Epitaxial Growth of Deposited Amorphous Layer by Laser Annealing," Appl. Phys. Lett. 33, 130 (1978).

19. A. C. Greenwald, A. R. Kirkpatrick, R. G. Little, and J. A. Minnucci, "Pulsed-Electron-Beam Annealing of Ion-Implantation Damage," J. Appl. Phys. 50, 783 (1979).

20. K. Kajiyama, Y. Mizushima, and S. Sakatu, "Schottky Barrier Height of n-$In_xGa_{1-x}As$ Diodes," Appl. Phys. Lett. 23, 458 (1973).

21 J. G. Ruch, "Electron Dynamics in Short Channel Field-Effect Transistors," IEEE Trans. ED-19, 652 (1972).

22. J. S. Escher, P. E. Gregory, S. B. Hyder, and R. Sankaran, "Transferred-Electron Photoemission to 1.65 μm from InGaAs," J. Appl. Phys. 49, 2591 (1978).

23. J. R. Hauser, "Avalanche Breakdown Voltages for III-V Semiconductors," Appl. Phys. Lett. 33, 351 (1978).

24. H. Morkoc, S. G. Bandy, R. Sankaran, G. A. Antypas, and R. L. Bell, "A Study of High-Speed Normally-Off and Normally-On $Al_{0.5}Ga_{0.5}As$ Heterojunction Gate GaAs FET's (HJFET)," IEEE Trans. ED-25, 619 (1978).

APPENDIX A:

EFFECTIVE SATURATED DRIFT VELOCITY DETERMINATION

Although there are various theories describing the drain characteristics of the FET obtained by joining the Shockley gradual channel approximation region near the source end of the channel to a velocity saturated region near the drain end of the channel, it will be assumed for this study that the entire channel is velocity saturated everywhere under the gate. It has been found that for the short gate length devices fabricated (around one micron or less) both the transconductance (g_m) and the drain current (I_d) are quire accurately described by the expressions resulting from this assumption, and the resulting analysis will be greatly simplified.

The relationship between this effective saturated drift velocity, v_s, and the velocity values shown on a velocity-field characteristic is not straightforward because of velocity overshoot. Accordingly, v_s will simply afford an empirical basis of comparison between InGaAsP and GaAs. For the sake of analysis, it will be assumed that the gate length (L) is short enough so that the electric field is constant throughout the channel at a value above the peak field. Consequently, carrier accumulation and depletion regions are nonexistent meaning that the mobile electron charge (n) is equal to the channel doping (N_D) throughout the channel. With v_s and n constant along the channel, the gate depletion depth (w) must also be constant as shown in Fig. A-1 to maintain current continuity. For the general case of v_s and N_D varying with x, I_d can thus be written as

$$I_d = qZ \int_w^d N_D(x) v_s(x) dx \qquad \text{(A-1)}$$

where Z is the gate width. Thus with V_g as the gate voltage

$$g_m = \frac{\partial I_d}{\partial V_g} = qZ \frac{\partial}{\partial V_g} \int_w^d N_D(x) v_s(x) dx$$

$$= qZ \left[N_D(d) v_s(d) \frac{\partial d}{\partial V_g} - N_D(w) v_s(w) \frac{\partial w}{\partial V_g} + \int_w^d \frac{\partial (N_D(x) v_s(x))}{\partial V_g} dx \right]$$

$$= -qZ N_D(w) v_s(x) \frac{\partial w}{\partial V_g} \qquad \text{(A-2)}$$

by application of Leibnitz' rule.

Another relationship can be developed by differentiating Eq. (A-1) with respect to w and again applying Leibnitz' rule. This simply involves replacing V_g by w in Eq. (A-2), giving

$$\frac{\partial I_d}{\partial w} = - qZ N_D(w) v_s(w) \quad . \qquad \text{(A-3)}$$

If the doping is constant with x, then

$$w = \sqrt{\frac{2\varepsilon(\phi_B - V_g)}{qN_D}} \qquad \text{(A-4)}$$

and Eq. (A- 3) becomes

$$\frac{\partial I_D}{\partial (\sqrt{\phi_B - V_g})} = -\sqrt{2\varepsilon q N_D}\, Z v_s(w) \quad . \qquad \text{(A-5)}$$

Equation (A-5) reveals that if I_D is plotted as a function of $\sqrt{\phi_B - V_g}$, the resulting slope will be proportional to v_s so that a profile of v_s across the channel thickness can be obtained in much the same manner as a mobility profile can be obtained.

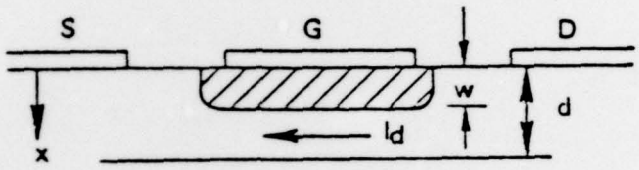

Figure A-1 Assumed channel profile.

APPENDIX B

This appendix represents a compendium of y-parameter data for some of the devices.

PAGE 3: ANA#5209/DEPT 0810 4/23/79
VARIAN METROLOGY LAB/C. NISHIMOTO
ING

.00 VOLTS, .00 MA (MEAS 1) ING 64-1

FREQ (MHZ)	GA MAX DB	GU MAX DB	S21 DB	S12 DB	K MAG	U MAG
2000.000			1.06	-40.94	.05	10.53
2500.000			1.10	-38.95	.17	3.65
3000.000			.85	-38.87	.19	2.52
3500.000			1.44	-37.85	.08	3.41
4000.000			1.60	-36.99	.13	1.83
4500.000		19.13	.72	-37.14	.30	.92
5000.000		15.16	1.11	-36.94	.88	.32
5500.000	13.40	12.70	.22	-34.27	1.42	.26
6000.000		16.87	.99	-35.37	.54	.62
6500.000		17.21	1.23	-36.77	.58	.56
7000.000		17.31	.98	-39.08	.53	.45
7500.000		16.54	.96	-40.26	.62	.33
8000.000		16.76	1.11	-39.24	.29	.38
8500.000		13.98	-.81	-36.64	.43	.33
9000.000		14.98	-.43	-34.63	.07	.50
9500.000		15.20	-.51	-31.90	-.11	.73
10000.00			-1.83	-29.62	-.25	1.01
10500.00			-.71	-27.59	-.39	1.56
11000.00			-1.81	-26.21	-.40	1.85
11500.00			-1.73	-24.78	-.26	1.25
12000.00			-1.57	-22.89	-.33	1.76
12500.00			-2.35	-21.05	-.16	1.88
13000.00			-2.76	-18.98	-.35	1.61
13500.00			-3.01	-18.70	-.50	3.06
14000.00			-3.77	-15.43	-.40	3.19

REF PLANE EXT(CM): IN= 2.70, OUT= 2.70

3C 2 INCH - (Cr)

ING 64-1: V_d = 4.V V_g = 0V

- Shorted -

	y_{11}		y_{21}		y_{12}		y_{22}	
2.00	.07831	2.24263	11.48909	-1.61469	.01280	-.09110	.28629	1.34571
2.50	.19497	2.78819	11.71991	-1.85625	.01833	-.11735	.38264	1.65740
3.00	.30792	3.51956	11.47685	-2.02370	.02084	-.11818	.39040	2.00841
3.50	.29123	4.16483	12.28162	-2.61054	.03290	-.13196	.34348	2.44356
4.00	.45670	5.22006	12.90861	-2.74381	.04790	-.14741	.48964	3.09145
4.50	.76497	6.23021	11.87413	-3.18166	.06386	-.14343	.63959	3.69041
5.00	2.22119	8.26958	13.42731	-4.62339	.11202	-.13833	.67098	3.80330
5.50	2.33388	8.33813	11.42476	-4.61590	.07553	-.21936	.87094	4.09746
6.00	.98288	6.20565	12.35790	-4.48791	.08767	-.17976	.83021	4.70857
6.50	1.05605	7.51415	12.95530	-4.97307	.08750	-.15155	.83536	5.27465
7.00	1.08013	8.79694	12.85819	-5.13504	.10093	-.09412	.82460	5.85134
7.50	1.36459	9.70958	13.07466	-5.82121	.11724	-.04037	.90268	6.42268
8.00	1.48679	10.57903	13.56380	-6.38490	.14181	.02501	.85711	6.98056
8.50	2.08222	11.80883	11.43942	-5.33429	.18636	.08297	.92889	7.56519
9.00	2.22218	12.60258	12.13282	-5.91757	.19849	.17254	.85337	8.11263
9.50	2.36752	13.42687	12.28074	-6.25735	.21807	.30015	.91901	8.74394
10.00	2.30350	14.54371	11.62812	-6.71350	.26496	.42402	.81665	9.33424

VARIAN METROLOGY LAB/C. NISHIMOTO

ING

.00 VOLTS, .00 MA (MEAS 1) ING64-2

FREQ (MHZ)	GA MAX DB	GU MAX DB	S21 DB	S12 DB	K MAG	U MAG
2000.000			-.49	-39.48	.27	2.07
2500.000			-.58	-36.75	.47	1.07
3000.000		17.05	-.79	-35.41	.59	.81
3500.000			-.16	-34.55	.47	1.06
4000.000		16.22	-.18	-33.91	.62	.72
4500.000		14.21	-.96	-33.41	.85	.52
5000.000	16.23	13.65	-.46	-33.44	1.00	.42
5500.000	13.71	12.70	-.67	-33.43	1.20	.34
6000.000	13.13	12.30	-.54	-33.75	1.34	.29
6500.000	12.90	12.15	-.33	-34.42	1.49	.25
7000.000	12.18	11.45	-.62	-35.09	1.76	.20
7500.000	11.29	10.67	-.62	-36.07	2.32	.14
8000.000	11.16	10.50	-.48	-37.45	2.79	.11
8500.000	8.82	8.32	-2.16	-38.41	4.32	.07
9000.000	8.98	8.38	-1.91	-39.71	4.96	.06
9500.000	9.27	8.19	-2.11	-35.20	2.77	.10
10000.00	9.86	8.22	-2.31	-32.90	1.89	.13
10500.00	11.00	8.54	-2.01	-31.08	1.35	.17
11000.00	10.50	7.90	-2.35	-29.58	1.27	.18
11500.00	7.97	6.37	-2.78	-28.61	1.72	.13
12000.00	7.53	5.95	-2.61	-27.21	1.67	.13
12500.00	4.82	3.94	-3.47	-26.54	2.45	.09
13000.00	6.20	4.74	-3.78	-25.24	1.60	.13
13500.00		7.15	-4.18	-22.61	.41	.35
14000.00	2.92	-.08	-8.38	-16.88	1.85	.20

REF PLANE EXT(CM): IN= 2.70, OUT= 2.70

ING 64-2, V_d = 4V

	y_{11}		y_{22}		y_{12}		y_{22}	
10.502	.16528	3.15367	9.98355	-1.58124	.00900	-.12869	.92459	1.27258,
11.0015	.27010	3.86257	10.15140	-1.78997	.01386	-.15839	1.04793	1.55362,
11.503	.42088	4.81062	9.94874	-2.11467	.02303	-.18759	1.10000	1.90526,
12.003	.38764	5.54346	10.74438	-2.48054	.02923	-.20796	1.09154	2.22800,
12.504	.58255	6.65857	11.12056	-2.77267	.04063	-.23045	1.17063	2.75783,
13.004	.78564	7.47483	10.22167	-2.93388	.04411	-.25014	1.21747	3.01365,
13.504	1.04076	8.47634	11.02002	-3.79450	.05426	-.25530	1.32453	3.45001,
14.004	1.30725	9.30159	10.92476	-4.19362	.06962	-.25983	1.38484	3.80482,
14.506	1.47941	10.52655	11.34706	-4.81654	.08343	-.25679	1.34199	4.38944,
15.006	1.61866	11.51880	11.92908	-5.31117	.09665	-.23921	1.41926	4.94454,
15.507	2.02630	12.79353	11.86828	-5.78562	.12072	-.21778	1.47786	5.51544,
16.007	2.42291	13.74102	12.30658	-6.27052	.13364	-.19086	1.62745	6.07374,
16.508	2.87377	14.78429	12.77994	-7.08404	.15622	-.13580	1.64555	6.59995,
17.008	3.51703	16.54634	11.13535	-6.42900	.16972	-.10198	1.66114	7.15168,
17.509	4.07439	17.65071	11.45315	-7.78585	.17530	.03091	1.74585	7.56269,
18.009	5.05034	18.84811	11.60165	-8.12356	.27978	.14255	1.72130	8.09803,
18.510	5.52449	20.61769	11.19574	-9.39434	.36231	.23528	1.67549	8.61967,

VARIAN METROLOGY LAB/C. NISHIMOTO

ING

.00 VOLTS, .00 MA (MEAS 1) ING 65-1 VD=4V

FREQ (MHZ)	GA MAX DB	GU MAX DB	S21 DB	S12 DB	K MAG	U MAG
2000.000	15.34	14.61	-4.99	-42.92	1.37	.32
2500.000	12.74	12.25	-5.00	-41.68	1.95	.21
3000.000	11.79	11.25	-5.01	-40.58	2.11	.19
3500.000	12.85	12.00	-4.80	-40.10	1.68	.23
4000.000	11.10	10.50	-4.75	-40.39	2.45	.15
4500.000	9.64	9.16	-5.00	-41.52	3.71	.10
5000.000	9.36	8.62	-4.86	-40.62	3.63	.09
5500.000	8.70	7.88	-5.01	-39.59	3.68	.09
6000.000	8.44	7.46	-5.10	-38.39	3.38	.09
6500.000	7.87	6.94	-5.32	-37.75	3.49	.09
7000.000	8.23	6.52	-5.63	-32.95	1.89	.15
7500.000	7.81	5.93	-5.83	-31.12	1.69	.16
8000.000	7.49	5.35	-6.11	-29.34	1.48	.17
8500.000	7.13	4.71	-6.50	-27.77	1.34	.18
9000.000	7.05	4.26	-6.79	-26.80	1.24	.19
9500.000	7.96	4.16	-7.07	-25.83	1.05	.22
10000.00		3.63	-7.57	-24.83	.97	.22
10500.00		3.42	-7.75	-23.94	.89	.24
11000.00	6.01	2.34	-8.32	-23.22	1.06	.21
11500.00	3.07	1.08	-8.72	-22.75	1.44	.16
12000.00	1.12	-.25	-9.31	-22.08	1.83	.13
12500.00	-.33	-1.33	-9.70	-21.79	2.29	.10
13000.00	1.84	-.08	-9.74	-21.14	1.42	.16
13500.00	-1.45	-2.65	-11.05	-19.42	1.97	.12
14000.00	-2.83	-3.44	-10.04	-20.35	3.22	.07

REF PLANE EXT(CM): IN= 2.70, OUT= 2.70

ING 65-1, V_d=4V 2-2. InGaAs (T_c)

	y_{11}		y_{21}		y_{12}		y_{22}	
2.00	.38853	3.69664	5.95535	-1.37490	.01755	-.07600	.90187	1.93405
2.50	.56304	4.56556	6.06032	-1.62383	.02995	-.08699	1.05752	2.37522
3.00	.70270	5.73302	6.14617	-1.87907	.04008	-.09921	1.08489	2.98010
3.50	.58773	6.71834	6.32079	-2.17642	.05041	-.10336	1.08236	3.54064
4.00	.85421	8.12723	6.56307	-2.51933	.06619	-.09385	1.24064	4.32664
4.50	1.13083	9.20984	6.47612	-2.88336	.07363	-.07625	1.28504	4.79582
5.00	1.49653	10.64835	6.80117	-3.31715	.11404	-.04609	1.39347	5.58590
5.50	1.68219	11.96937	6.80192	-3.77036	.14421	-.01519	1.53088	6.14003
6.00	2.17209	13.71405	7.01334	-4.21404	.17375	.03377	1.51651	7.13461
6.50	2.44748	15.45238	7.02775	-4.74028	.15776	.12775	1.68949	7.94643
7.00	3.02478	17.15437	7.22838	-4.87560	.26517	.26517	1.56717	8.88784
7.50	3.33769	18.92699	7.39199	-5.27059	.34525	.35751	1.71703	9.78778
8.00	4.00088	20.58276	7.46640	-5.80339	.40264	.51536	1.87505	10.68375
8.50	4.76097	22.39960	7.56862	-6.12895	.54123	.64501	2.02109	11.46618
9.00	5.51625	23.85350	7.46489	-6.72142	.68473	.73428	2.16904	12.30123
9.50	6.03274	26.13066	7.53796	-7.27933	.74495	.95049	2.03637	13.17680
10.00	7.51585	28.04952	7.05138	-8.11162	.90687	1.16074	1.99505	14.19143

PAGE 3: ANA=5209/DEPT 0810 4/23/79
VARIAN METROLOGY LAB/C. NISHIMOTO
ING

.00 VOLTS, .00 MA (MEAS 1) ING 65-2 VD=4V

FREQ (MHZ)	GA MAX DB	GU MAX DB	S21 DB	S12 DB	K MAG	U MAG
2000.000	12.14	12.61	-2.58	-46.19	4.68	.10
2500.000	9.50	9.89	-3.16	-45.22	7.14	.06
3000.000	8.03	8.29	-3.98	-45.97	9.92	.04
3500.000	7.55	7.77	-4.32	-46.34	11.12	.04
4000.000	5.92	6.08	-5.18	-47.40	16.52	.02
4500.000	-1.36	-1.29	-16.14	-55.02	60.13	.01
5000.000	-2.62	-2.64	-16.92	-60.57	139.12	.00
5500.000	-3.61	-3.70	-17.96	-48.67	39.41	.01
6000.000	-4.79	-4.91	-19.11	-44.31	27.43	.01
6500.000	-5.90	-6.07	-20.29	-38.66	16.13	.02
7000.000	-6.92	-7.18	-21.53	-35.91	12.91	.03
7500.000	-8.85	-9.12	-22.94	-33.56	13.04	.03
8000.000	-11.37	-11.57	-24.57	-31.82	15.78	.02
8500.000	-16.19	-16.31	-27.85	-29.31	24.60	.01
9000.000	-22.44	-22.51	-33.97	-26.69	37.94	.01
9500.000	-26.39	-26.44	-36.81	-25.78	61.16	.01
10000.00	-25.39	-25.45	-36.94	-24.53	41.47	.01
10500.00	-29.59	-29.61	-42.98	-23.87	50.43	.01
11000.00	-22.09	-21.98	-35.62	-23.25	19.45	.02
11500.00	-19.71	-19.55	-32.22	-22.54	15.30	.03
12000.00	-16.85	-16.55	-28.71	-21.54	10.64	.04
12500.00	-15.56	-15.25	-25.93	-20.50	9.67	.04
13000.00	-11.80	-11.15	-22.94	-18.93	4.82	.09
13500.00	-8.19	-6.86	-19.81	-17.02	2.49	.22
14000.00	-5.75	-4.10	-15.29	-13.34	1.75	.33

REF PLANE EXT(CM): IN= 2.70, OUT= 2.70

ING 65-2, Vd=4V [illegible] InGaAs (Tc)

— Shorted —

	y_{11}		y_{21}		y_{12}		y_{22}	
19.00	.82770	3.08903	6.28824	-5.46628	-.00192	-.05497	1.10771	2.74166
19.50	1.16592	3.58834	5.29895	-6.09579	-.00446	-.06384	1.39804	3.29357
20.00	1.36246	4.19321	4.21184	-6.24431	.00105	-.05999	1.45188	3.99900
20.50	1.51727	4.66969	3.45249	-6.49320	.00606	-.05769	1.42093	4.64764
21.00	1.76171	5.42197	2.69800	-6.35609	.00739	-.05246	1.58629	5.53205
21.50	.66149	4.70674	-.22668	-1.84614	.00718	-.01973	1.69186	5.90522
22.00	.75432	5.36725	-.30302	-1.71849	.01027	.00394	1.80733	6.74506
22.50	.82585	5.87625	-.24623	-1.55462	.02895	.03575	1.82143	7.30536
23.00	.82518	6.72053	-.24675	-1.39941	.02666	.07330	1.91636	8.30066
23.50	.91353	7.44013	-.22036	-1.24972	.04981	.14466	1.92734	9.06743
24.00	.87302	8.30625	-.17787	-1.12300	.06344	.20752	1.94530	10.00763
24.50	.95048	9.04319	-.19081	-.98163	.08131	.28357	2.09833	10.79495
25.00	1.22089	9.94333	-.16600	-.85402	.09145	.36677	2.28265	11.74321
25.50	1.65961	10.47839	-.21410	-.58825	.02769	.52828	2.51740	12.31350
26.00	1.75754	11.09668	-.06087	-.31314	.19075	.71189	2.52593	12.99478
26.50	2.37144	11.15675	.11587	-.20903	.30569	.79634	2.68335	13.80466
27.00	1.77584	11.21224	.18079	-.15170	.35335	.92051	2.60820	14.79167

.00 VOLTS, .00 MA (MEAS 1) ING 66-2 VD=4V

FREQ (MHZ)	GA MAX DB	GU MAX DB	S21 DB	S12 DB	K MAG	U MAG
2000.000	-2.16	-1.68	-18.60	-38.73	8.36	.06
2500.000	-4.78	-4.53	-19.58	-37.76	12.21	.03
3000.000	-5.88	-5.62	-20.58	-37.15	13.17	.03
3500.000	-6.72	-6.46	-21.25	-36.56	13.69	.03
4000.000	-7.58	-7.34	-21.87	-36.58	15.43	.03
4500.000	-8.16	-7.96	-22.29	-36.26	16.34	.03
5000.000	-9.24	-9.07	-22.81	-36.25	19.75	.02
5500.000	-10.71	-10.57	-23.90	-37.14	27.04	.01
6000.000	-10.66	-10.54	-24.23	-37.66	27.31	.01
6500.000	-11.89	-11.82	-25.09	-39.81	42.02	.01
7000.000	-12.51	-12.46	-25.94	-41.81	55.42	.01
7500.000	-14.23	-14.21	-27.18	-45.49	108.97	.00
8000.000	-15.47	-15.48	-28.42	-50.06	213.16	.00
8500.000	-16.57	-16.61	-29.82	-45.55	138.82	.00
9000.000	-18.66	-18.68	-32.13	-39.90	89.73	.00
9500.000	-23.39	-23.42	-36.81	-35.51	93.99	.00
10000.00	-26.40	-26.40	-40.51	-32.15	83.34	.00
10500.00	-23.74	-23.69	-37.82	-29.49	45.36	.01
11000.00	-18.94	-18.82	-32.79	-27.18	20.57	.02
11500.00	-18.14	-18.02	-30.30	-25.41	18.54	.02
12000.00	-17.48	-17.34	-28.76	-24.43	17.00	.02
12500.00	-16.06	-15.88	-25.89	-22.86	14.25	.02
13000.00	-12.41	-12.02	-22.26	-20.35	7.03	.05
13500.00	-7.55	-6.32	-18.30	-17.19	2.61	.20
14000.00	-4.36	-2.54	-12.32	-11.98	1.50	.39

REF PLANE EXT(CM): IN= 2.70, OUT= 2.70

ING 66-2, VD= 4V
2 μ InGaAs (C.-)

	y_{11}		y_{21}		y_{12}		y_{22}	
2.00	.43213	1.41342	.75883	-1.04444	-.04344	-.11934	1.41633	1.41
2.50	.61711	1.60763	.56917	-1.02680	-.04959	-.13526	1.58019	1.69
3.00	.65569	1.90427	.43114	-.96836	-.05336	-.14659	1.55203	2.05
3.50	.66427	2.17272	.34941	-.91024	-.05985	-.15591	1.55603	2.39
4.00	.70865	2.64470	.28206	-.87117	-.05253	-.16168	1.56334	2.94
4.50	.75679	2.82437	.24201	-.84399	-.05439	-.16739	1.60486	3.14
5.00	.81479	3.26796	.17423	-.81969	-.05735	-.16330	1.67568	3.59
5.50	.88519	3.55031	.14253	-.73328	-.06106	-.15113	1.71602	3.85
6.00	.87572	4.11996	.12555	-.71202	-.05769	-.14279	1.68866	4.42
6.50	.99008	4.65794	.10419	-.65780	-.04570	-.11312	1.79663	4.98
7.00	.91964	5.21554	.09543	-.60349	-.03986	-.08953	1.77777	5.47
7.50	1.00890	5.72173	.07515	-.53474	-.03379	-.05340	1.83259	5.99
8.00	1.03485	6.20921	.07431	-.46515	-.03730	.01140	1.85421	6.46
8.50	1.06047	6.69554	.08483	-.39906	-.00584	.06675	1.85237	6.91
9.00	1.00775	7.17053	.06030	-.31019	.00450	.12992	1.83667	7.36
9.50	1.07678	7.66170	.07945	-.17038	.01521	.21747	1.82773	7.91
10.00	.85546	8.13917	.11145	-.05434	.03949	.32153	1.79074	8.42

.00 VOLTS, .00 MA (MEAS 1) ING66-3 VD=3V

FREQ (MHZ)	GA MAX DB	GU MAX DB	S21 DB	S12 DB	K MAG	U MAG
2000.000	3.79	4.10	-15.04	-33.36	1.87	.26
2500.000	.29	.79	-15.07	-31.65	3.23	.14
3000.000	-.63	-.04	-15.02	-30.25	3.41	.13
3500.000	-1.41	-.86	-15.22	-29.77	3.77	.12
4000.000	-2.27	-1.76	-15.08	-28.82	4.16	.10
4500.000	-3.04	-2.50	-15.14	-28.24	4.61	.09
5000.000	-4.10	-3.66	-15.21	-28.05	5.68	.07
5500.000	-5.03	-4.63	-15.41	-27.64	6.55	.06
6000.000	-5.57	-5.21	-15.59	-27.75	7.35	.05
6500.000	-6.33	-6.02	-15.90	-28.04	8.72	.04
7000.000	-6.82	-6.53	-16.25	-28.26	9.61	.04
7500.000	-7.61	-7.38	-16.57	-28.89	11.94	.03
8000.000	-8.77	-8.62	-17.44	-31.09	18.14	.02
8500.000	-9.12	-8.99	-17.69	-32.14	21.55	.02
9000.000	-10.36	-10.27	-18.43	-33.57	31.03	.01
9500.000	-12.26	-12.21	-19.34	-33.64	43.67	.01
10000.00	-13.97	-13.95	-20.41	-35.90	74.15	.00
10500.00	-15.11	-15.11	-21.55	-48.97	380.87	.00
11000.00	-13.99	-13.99	-20.78	-40.74	124.89	.00
11500.00	-15.82	-15.84	-22.76	-34.32	72.33	.00
12000.00	-17.90	-17.92	-24.36	-31.01	66.27	.00
12500.00	-18.90	-18.92	-24.60	-31.09	81.95	.00
13000.00	-23.70	-23.72	-30.01	-25.68	71.13	.00
13500.00	-20.59	-20.53	-27.27	-20.33	25.76	.01
14000.00	-11.10	-11.14	-15.40	-14.93	6.15	.03

REF PLANE EXT(CM): IN= 2.70, OUT= 2.70

ING 66-3, V_d = 3V

22 ℃ Ambient

	h_{11}		h_{21}		h_{12}		h_{22}	
~~0.50~~	~~.35586~~	~~.22063~~	~~.15172~~	~~.09116~~	~~.00544~~	~~.02020~~	~~.01247~~	~~.14525~~
~~2.50~~	~~.32932~~	~~.24939~~	~~.13969~~	~~.10230~~	~~.00846~~	~~.02450~~	~~.79230~~	~~.15041~~
~~3.00~~	~~.90536~~	~~.25449~~	~~.12235~~	~~.12732~~	~~.01407~~	~~.02752~~	~~.78210~~	~~.20054~~
2.00	.18035	2.17569	1.84475	-.70814	-.03092	-.23909	1.98602	1.67426
2.50	.36909	2.62619	1.82440	-.85073	-.03644	-.29677	2.08667	2.08667
3.00	.45162	3.21342	1.75462	-1.05488	-.04774	-.34348	2.11091	2.51569
3.50	.57646	3.83963	1.67466	-1.12957	-.05261	-.37432	2.07520	2.95389
4.00	.69738	4.40311	1.65325	-1.29166	-.06742	-.42569	2.15904	3.57325
4.50	.83837	4.75465	1.57027	-1.41387	-.09709	-.45679	~~2.52793~~	~~3.91~~
5.00	1.14809	5.40133	1.43768	-1.55090	-.11878	-.47642	2.34407	4.40555
5.50	1.34498	5.82576	1.35493	-1.67320	-.14499	-.50562	2.36282	4.84450
6.00	1.52137	6.59064	1.30353	-1.72984	-.16502	-.50786	2.47662	5.56258
6.50	1.78974	7.17825	1.17206	-1.80482	-.18195	-.49992	2.51024	6.21305
7.00	1.81356	7.85537	1.08982	-1.81377	-.19392	-.49283	2.52342	6.93505
7.50	2.08779	8.37365	.95792	-1.88002	-.24774	-.44893	2.75360	7.5e54.
8.00	2.38502	8.90101	.80046	-1.79786	-.21065	-.35058	2.95984	8.13e10.
8.50	2.53379	9.47883	.85921	-1.76164	-.18550	-.22130	2.99848	8.70823.
9.00	2.83433	10.57785	.73575	-1.73331	-.15999	-.23862	3.25275	9.44668.
9.50	3.33245	10.89996	.67542	-1.67171	-.18953	-.29186	3.99518	9.88842.
10.00	4.07517	11.19644	.53784	-1.56200	-.27796	.00485	4.18903	9.8e6.2.

VARIAN METROLOGY LAB/C. NISHIMOTO

ING

.00 VOLTS, .00 MA (MEAS 1) ING 67-1 VD=4V

FREQ	Y11		Y21		Y12		Y22	
(MHZ)	MAG	ANG	MAG	ANG	MAG	ANG	MAG	ANG
2000.000	1.681	88	.552	-40	.066	-89	2.723	49
2500.000	2.046	86	.529	-45	.077	-88	3.157	53
3000.000	2.575	87	.523	-45	.090	-89	3.695	58
3500.000	3.036	88	.494	-40	.077	-97	4.153	62
4000.000	3.773	88	.505	-38	.076	-78	4.902	66
4500.000	4.161	88	.509	-38	.070	-73	5.337	68
5000.000	4.862	87	.509	-35	.059	-60	6.114	69
5500.009	5.386	87	.499	-33	.044	-39	6.680	71
6000.000	6.274	87	.493	-28	.044	13	7.634	73
6500.000	6.964	87	.480	-22	.068	40	8.452	74
7000.000	7.816	88	.470	-13	.128	68	9.405	75
7500.000	8.529	87	.484	-4	.208	73	10.211	76
8000.000	9.322	87	.512	6	.321	77	11.129	76
3500.000	10.104	87	.533	11	.417	73	11.841	78
9000.000	10.837	87	.577	24	.543	75	12.720	78
9500.000	11.705	87	.694	36	.681	73	13.602	79
10000.00	12.566	85	.860	41	.832	72	14.505	79
10500.00	12.523	82	.977	41	.949	71	15.415	80
11000.00	12.757	85	1.034	47	1.098	74	16.497	80
11500.00	13.358	85	1.190	53	1.305	75	17.107	79
12000.00	14.013	85	1.467	59	1.620	76	18.195	78
12500.00	14.436	85	1.823	62	1.982	76	18.654	78
13000.00	15.137	86	2.406	65	2.582	75	19.495	79
13500.00	16.498	83	3.938	56	4.097	64	20.917	78
14000.00	13.743	74	3.840	5	4.250	2	18.630	67

REF PLANE EXT(CM): IN= 2.70, OUT= 2.70

ING 67-1, V 4V 22? [illegible] (Tc)

	y_{11}		y_{21}		y_{12}		y_{22}	
10.50	.05867	1.67998	.36936	-.41022	.00115	-.06599	1.78645	2.05507·
1..00	.14272	2.04102	.37406	-.37406	.00265	-.07695	1.89993	2.52127·
:.50	.13477	2.57147	.36982	-.36982	.00157	-.08999	1.93421	3.09588·
.50	.10595	3.03415	.37843	-.31754	-.00938	-.07643	1.94973	3.06695·
~~.50~~	~~.10595~~	~~3.03415~~	~~.37843~~	~~-.31754~~	~~-.00938~~	~~-.07643~~	~~1.94972~~	~~[illegible]~~
.00	.13168	3.77070	.39795	-.31091	.01580	-.07434	1.99382	4.47520·
.50	.14522	4.15847	.40110	-.31337	.02047	-.06694	1.99928	4.94688·
.00	.25446	4.85534	.41695	-.29195	.02950	-.05110	2.19106	5.70791·
.50	.28188	5.37862	.41850	-.27177	.03419	-.02769	2.17480·	6.31606·

.08727732238112426544579543561057323148479504281868009434192399084830043·

1.1	.3254	6.2654	.4353	-.2314	.0429	0099	2.232	7.3064
6.5	.3645	6.9545	.4456	-.1798	.0521	.0437	2.3297	8.1246

7.00	.27277	7.81124	.45795	-.10573	.04795	.11868	2.43419	9.08453·
7.50	.44637	8.51731	.48882	-.03376	.06081	.19891	2.47026	9.89769·
.00	.48788	9.30922	.50920	.05252	.07221	.31277	2.69235	10.79942·
.50	.52880	10.09015	.52321	.10170	.12046	.39400	2.46189	11.58225·
.00	.56716	10.82215	.52712	.23469	.14054	.52450	2.64464	12.44204·
.50	.61259	11.68896	.56146	.40792	.19911	.65124	2.59508	13.35207·
.00	1.09520	12.51818	.64905	.56421	.25710	.79128	2.76768	14.23650·

PAGE 3: ANA=5209/DEPT 0810 4/23/79
VARIAN METROLOGY LAB/C. NISHIMOTO
ING

.00 VOLTS, .00 MA (MEAS 1) ING 67-2 VD=3V

FREQ (MHZ)	GA MAX DB	GU MAX DB	S21 DB	S12 DB	K MAG	U MAG
2000.000	-.20	.05	-17.47	-45.72	13.55	.03
2500.000	-3.37	-3.22	-19.87	-45.04	21.59	.02
3000.000	-4.32	-4.17	-20.31	-44.53	22.02	.02
3500.000	-4.94	-4.78	-21.42	-44.61	22.50	.02
4000.000	-6.20	-6.11	-22.35	-45.53	30.07	.01
4500.000	-7.04	-6.91	-23.01	-47.21	41.03	.01
5000.000	-8.67	-8.64	-23.92	-50.85	81.80	.00
5500.000	-10.04	-10.01	-24.89	-60.51	304.57	.00
6000.000	-10.40	-10.46	-25.93	-48.50	73.75	.01
6500.000	-11.87	-11.94	-27.16	-43.08	48.09	.01
7000.000	-12.33	-12.44	-28.14	-39.70	32.34	.01
7500.000	-14.96	-15.04	-30.01	-36.17	31.87	.01
8000.000	-16.11	-16.20	-31.23	-33.53	26.58	.01
8500.000	-16.69	-16.78	-32.37	-31.89	22.11	.02
9000.000	-17.53	-17.53	-33.30	-29.31	17.89	.02
9500.000	-16.55	-16.49	-32.42	-27.87	13.38	.03
10000.00	-14.55	-14.26	-30.93	-26.32	8.41	.05
10500.00	-12.13	-11.61	-28.27	-24.62	5.41	.08
11000.00	-10.83	-10.21	-26.47	-23.45	4.34	.11
11500.00	-11.64	-11.17	-25.34	-22.93	5.57	.08
12000.00	-11.43	-10.96	-24.42	-22.65	5.72	.07
12500.00	-11.55	-11.12	-22.92	-22.62	6.94	.06
13000.00	-8.68	-7.69	-20.90	-20.87	3.43	.14
13500.00	-6.57	-4.97	-18.35	-17.40	2.16	.27
14000.00	-5.17	-3.43	-14.66	-13.96	1.68	.35

REF PLANE EXT(CM): IN= 2.70, OUT= 2.70

67-2

ING 67-2 VD= 3V 22 InGaAs (Te)

	y_{11}		y_{21}		y_{12}		y_{22}	
10.50	.30493	1.72932	.48770	-1.41639	-.01501	-.05602	1.90257	2.18656
11.00	.40566	2.08694	.37102	-1.21355	-.01221	-.06282	2.07355	2.65402
11.50	.40391	2.55021	.34146	-1.05093	-.01064	-.06716	2.05238	3.28449
12.00	.36536	2.97565	.31808	-.92377	-.00993	-.06774	2.04455	3.84524
12.50	.38414	3.65487	.30577	-.84009	-.00216	-.06196	2.17352	4.66114
13.00	.41979	3.99400	.28593	-.78558	.00181	-.05197	2.18888	5.15667
13.50	.47704	4.62525	.27630	-.71979	.00548	-.03457	2.29678	5.96332
14.00	.53038	5.04820	.26260	-.64935	.00787	-.00906	2.38354	6.54872
14.50	.47223	5.87218	.27837	-.57073	.01761	.04358	2.43505	7.49403
15.00	.56573	6.46630	.28250	-.48930	.03371	.08345	2.39887	8.26586
15.50	.50273	7.18944	.30388	-.41826	.04234	.13029	2.50330	9.34243
16.00	.54696	7.82190	.28773	-.31953	.08309	.11878	2.53050	10.14969
16.50	.59049	8.44436	.31537	-.22033	.06636	.28744	2.74799	11.02159
17.00	.47552	9.07355	.31609	-.14073	.07589	.35702	2.73855	11.86196
17.50	.47102	8.98767	.31956	.01675	.07042	.50103	2.70992	12.74918
18.00	.54267	10.35479	.33242	.13673	.09652	.60940	2.89870	13.62120
18.50	.38494	11.02328	.32692	.30485	.10591	.75359	2.83790	14.59974

PAGE 3: ANA=5209/DEPT 0810 4/23/79
VARIAN METROLOGY LAB/C. NISHIMOTO
ING

.00 VOLTS, .00 MA (MEAS 1) ING 68-1 VD=4V

FREQ (MHZ)	GA MAX DB	GU MAX DB	S21 DB	S12 DB	K MAG	U MAG
2000.000			5.08	-38.38	.28	2.76
2500.000			5.05	-36.74	.42	1.43
3000.000			5.02	-35.96	.46	1.23
3500.000			5.15	-34.93	.41	1.45
4000.000		20.60	5.20	-34.67	.57	.95
4500.000		19.98	5.06	-34.38	.55	.85
5000.000		18.71	5.11	-34.33	.70	.62
5500.000		17.97	5.06	-34.61	.81	.50
6000.000		17.46	4.96	-34.78	.87	.43
6500.000	19.14	17.01	4.91	-35.78	1.04	.35
7000.000	17.89	16.54	4.72	-37.41	1.28	.26
7500.000	16.95	15.81	4.56	-39.03	1.69	.18
8000.000	16.92	15.45	4.43	-39.89	1.82	.15
8500.000	17.03	15.06	4.81	-39.50	1.65	.15
9000.000	18.02	14.95	3.99	-37.62	1.21	.19
9500.000		14.73	3.79	-35.41	.87	.23
10000.00		14.66	3.61	-33.10	.55	.31
10500.00		14.72	3.55	-30.98	.32	.40
11000.00		14.49	3.32	-29.16	.21	.48
11500.00		14.02	3.06	-27.39	.15	.54
12000.00		13.80	2.85	-25.64	.08	.64
12500.00		13.25	2.42	-23.55	.02	.75
13000.00			2.14	-20.46	-.36	2.77
13500.00			.62	-15.60	-.44	4.32
14000.00		7.06	2.11	-19.10	.81	.19

REF PLANE EXT(CM): IN= 2.70, OUT= 2.70

68-1

ING 68-1 VD = 4V 25°C Unbias

	y_{11}	y_{21}		y_{12}		y_{22}	
2.00	.15481	2.95395	19.27227 -2.36634	-.00227	-.12398	1.19423	1.0[illegible]
2.50	.31690	3.62216	19.51573 -3.09033	-.00281	-.16098	1.32583	1.3[illegible]
3.00	.39333	4.49583	19.70934 -3.47539	.00316	-.18097	1.35556	1.6[illegible]
3.50	.36399	5.20529	20.10274 -3.90758	.00703	-.20238	1.35940	2.0[illegible]
4.00	.35283	6.31886	20.79131 -4.41987	0.00000	-.21600	1.42776	2.5[illegible]
4.50	.73201	6.96464	20.54814 -5.50536	.02766	-.22531	1.47508	2.7[illegible]
5.00	.98227	7.99998	21.33675 -6.10675	.03284	-.23370	1.58559	3.25[illegible]
5.50	1.07708	8.77212	21.49363 -6.98533	.04484	-.23068	1.67906	3.60[illegible]
6.00	1.22332	9.96318	21.73791 -7.91195	.06160	-.22989	1.69659	4.19[illegible]
6.50	1.34953	10.99146	22.23882 -8.53666	.06491	-.21230	1.82983	4.76[illegible]
7.00	1.70974	12.16544	22.23664 -9.43839	.08285	-.16987	1.83652	5.33[illegible]
7.50	2.07745	13.11630	22.61756-10.06999	.10542	-.12563	2.02927	5.89[illegible]
8.00	2.24796	14.19308	22.74483-11.09342	.13722	-.06991	2.08401	6.41[illegible]
8.50	2.70561	15.34429	22.31526-11.37019	.16697	-.00291	2.11999	6.9[illegible]
9.00	2.87926	16.32910	22.63866-12.54861	.20203	.07353	2.14253	7.47[illegible]
9.50	3.07600	17.44488	22.81544-13.17250	.23673	.16576	2.17020	8.0[illegible]
10.00	3.61696	18.60772	22.81419-14.25589	.27789	.27789	2.16327	8.5[illegible]

PAGE 3: ANA#5209/DEPT 0810 4/23/79
VARIAN METROLOGY LAB/C. NISHIMOTO
ING

.00 VOLTS, .00 MA (MEAS 1) ING 68-2 VD=4V

FREQ (MHZ)	GA MAX DB	GU MAX DB	S21 DB	S12 DB	K MAG	U MAG
2000.000			4.73	-36.93	.35	1.91
2500.000			4.75	-35.37	.49	1.25
3000.000			4.79	-34.29	.47	1.16
3500.000			4.90	-33.42	.50	1.12
4000.000		19.54	5.00	-32.59	.50	.94
4500.000		19.04	5.00	-32.02	.55	.89
5000.000		17.67	5.04	-31.74	.68	.64
5500.000		16.99	5.05	-31.59	.77	.54
6000.000		16.35	4.97	-31.84	.90	.45
6500.000	17.13	15.65	4.95	-32.87	1.09	.35
7000.000	15.90	15.28	4.76	-34.27	1.37	.26
7500.000	15.22	14.53	4.58	-36.45	1.84	.17
8000.000	15.23	14.12	4.40	-36.66	1.84	.15
8500.000	14.81	13.63	3.94	-37.31	2.04	.13
9000.000	15.22	13.57	3.89	-37.28	1.86	.13
9500.000	15.90	13.25	3.57	-34.75	1.30	.17
10000.00		12.95	3.28	-31.77	.81	.23
10500.00		12.33	2.99	-28.68	.53	.28
11000.00	13.76	11.30	3.28	-30.57	1.28	.16
11500.00	13.50	11.77	3.31	-33.09	1.65	.14
12000.00		11.99	3.13	-29.88	.95	.22
12500.00		11.51	2.78	-27.26	.72	.27
13000.00		14.21	2.58	-24.50	.00	.80
13500.00			2.02	-20.68	-.48	
14000.00			-2.29	-13.54	-.43	16.78

REF PLANE EXT(CM): IN= 2.70, OUT= 2.70

ING 68-2 Vd = 4V 25% Int A

2.30	.20959	2.73854	18.64656	-2.28956	-.00541	-.15491	1.31289	.75800
2.00	.35289	3.35751	19.00919	-2.67157	-.01318	-.18854	1.45745	.96700
1.50	.44351	4.21976	19.26087	-3.39621	.00379	-.21697	1.44829	1.25699
1.00	.51940	4.94178	19.64512	-4.17570	.00426	-.24396	1.49490	1.54302
.50	.73451	5.98208	20.36302	-4.33831	.01913	-.27433	1.58861	2.02633
.00	.70881	6.74385	20.57318	-5.12947	.02096	-.29887	1.57045	2.24284
1.50	1.09293	7.77658	21.25830	-6.09572	.03345	-.31885	1.68726	2.70019
1.00	1.21081	8.61533	21.64795	-7.03364	.04083	-.33250	1.76400	3.05134
2.50	1.56951	9.90948	22.13728	-7.82936	.03533	-.33615	1.78286	3.65540
2.00	1.75754	11.09668	22.71868	-8.72088	.04056	-.30995	1.89987	4.25711
3.50	2.19383	12.43615	23.07112	-9.32134	.05304	-.27239	1.93694	4.64361
3.00	2.64022	13.58278	23.35662	-10.39904	.09951	-.20403	2.09000	5.44464
4.50	3.13531	14.75047	23.55110	-11.48664	.16116	-.16689	2.18072	5.99149
5.00	3.41578	16.06999	23.08954	-11.76471	.18996	-.11870	2.13036	6.55633
5.50	4.00030	17.31722	23.54476	-13.05107	.23434	.00410	2.16940	7.09578
6.00	4.69619	18.83538	23.71437	-13.69130	.31914	.09151	2.13573	7.65741
6.5	5.7421 y_{11} 20.525		23.9304 y_{21} -14.3824		.4471 y_{12}	.2088	2.2082 y_{22}	8.2413

ING 68-2 Vd = 4V

RCA
Microwave Technical Center
Dr. F. Sterzer
Princeton, NJ 08540

Hewlett-Packard Corp.
Dr. Robert Archer
1501 Page Mill Road
Palo Alto, CA 94306

Watkins-Johnson Co.
E. J. Crescenzi, Jr./
K. Niclas
3333 Hillview Avenue
Stanford Industrial Park
Palo Alto, CA 94304

Commandant
Marine Corps
Scientific Advisor (Code AX)
Washington, D.C. 20380

Communications Transistor Corp.
Dr. W. Weisenberger
301 Industrial Way
San Carlos, CA 94070

Microwave Associates
Northwest Industrial Park
Drs. F. A. Brand/J. Saloom
Burlington, MA 01803

Commander, AFAL
AFAL/DHM
Mr. Richard L. Remski
Wright-Patterson AFB, OH 45433

Professor Walter Ku
Phillips Hall
Cornell University
Ithaca, NY 14853

Commander
Harry Diamond Laboratories
Mr. Horst W. A. Gerlach
2800 Powder Mill Road
Adelphia, MD 20783

Advisory Group on Electron
Devices
201 Varick Street, 9th floor
New York, NJ 10014

D. Claxton
MS/1414
TRW Systems
One Space Park
Redondo Beach, CA 90278

Professor L. Eastman
Phillips Hall
Cornell University
Ithaca, NY 14853

Dr. W. Wisseman, MS 118
Texas Instruments
P. O. Box 225936
Dallas, TX 75265

AIL TECH
612 N. Mary Avenue
Sunnyvale, CA 94086
Attn: G. D. Vendelin

Profs. Hauser and Littlejohn
Department of Electrical Engr.
North Carolina State University
Raleigh, NC 27607

DISTRIBUTION LIST - TECHNICAL REPORTS

Contract N00014-78-C-0380

Code 427
Office of Naval Research
Arlington, VA 22217

Naval Research Laboratory
4555 Overlook Avenue, S.W.
Washington, D.C. 20375
Code 5211
Code 5250

Defense Documentation Center
Building 5, Cameron Station
Alexandria, VA 22314

Dr. Y. S. Park
AFAL/DHR
Building 450
Wright-Patterson AFB
Ohio, 45433

ERADCOM
DELET-M
Fort Monmouth, NJ 07703

Texas Instruments
M.S. 105/W. Wisseman
P. O. Box 5936
Dallas, TX 75222

Commanding Officer
Office of Naval Research
Branch Office
1030 East Green Street
Pasadena, CA 91101

Mr. M. Malbon
Avantek, Inc.
3175 Bowers Avenue
Santa Clara, CA 94304

Mr. R. Bierig
Raytheon Company
28 Seyon Street
Waltham, MA 02154

Dr. R. Bell, K-101
Varian Associates, Inc.
611 Hansen Way
Palo Alto, CA 94304

Dr. H. C. Nathanson
Westinghouse Research and
Development Center
Beulah Road
Pittsburgh, PA 15235

Dr. F. Blum/Dr. Daniel Chen
Rockwell International
Science Center
P. O. Box 1085
Thousand Oaks, CA 91360

Mr. G. J. Gilbert
MSC
100 Schoolhouse Road
Somerset, NJ 08873

Dr. C. Krumn
Hughes Research Laboratory
3011 Malibu Canyon Road
Malibu, CA 90265

Mr. Lothar Wandinger
ECOM/AMSEL/TL/IJ
Fort Monmouth, NJ 07003

Dr. Harry Wieder
Naval Ocean Systems Center
Code 922
271 Catalina Blvd.
San Diego, CA 92152

Dr. William Lindley
MIT
Lincoln Laboratory
F124A, P. O. Box 73
Lexington, MA 02173

Mr. Sven Roosild
AFCRL/LQD
Hanscom AFB, MA 01731

Commander
US Army Electronics Command
V. Gelnovatch
(DRSEL-TL-IC)
Fort Monmouth, NJ 07703